AN EXPERIMENTAL STUDY OF A VANE CONTROLLED JET FLAP GUST ALLEVIATION SYSTEM

Leonard Joseph Deal

Bibliography

Produced Wednesday, April 13, 2011 at 9:38 AM

Personal author: Deal, Leonard Joseph.
Title: An experimental study of a vane controlled jet flap
gust alleviation system.
Physical description: p. ; cm.
General note: AD777987.
Dissertation note: Thesis (Degree of A.E.)--Naval Postgraduate School,
1974.
Bibliography note: Bibliography: l. 73-74.
Subject: Aeronautics.

NAVAL POSTGRADUATE SCHOOL
Monterey, California

THESIS

AN EXPERIMENTAL STUDY OF A VANE CONTROLLED

JET FLAP GUST ALLEVIATION SYSTEM

by

Leonard Joseph Deal, Jr.

Thesis Advisor: M. F. Platzer

March 1974

An Experimental Study of a Vane Controlled Jet Flap Gust Alleviation System

by

Leonard Joseph Deal, Jr.
Lieutenant, United States Navy
B.S.A.E., Auburn University, 1966

Submitted in partial fulfillment of the
requirements for the degree of

AERONAUTICAL ENGINEER

from the

NAVAL POSTGRADUATE SCHOOL
March 1974

Author: Leonard J. Deal Jr.

Approved by: Max F. Platzer
Thesis Advisor

Ronald O. Ries
Second Reader

Chairman, Department of Aeronautics

Academic Dean

ABSTRACT

An experimental effort to demonstrate the feasibility of an active gust alleviator using a fluidically actuated jet flap control system was undertaken. The wing model had a variable deflection jet at the trailing edge and was free to move in pitch only. A vane mounted ahead of the wing served as gust sensor and provided the signal which controlled jet angle.

Experimental results showed the system capable of alleviating up to 92% of the motion caused by a sinusoidal gust at constant amplitude. RMS values of wing rotation angle were found to be 0.68 degrees with control off and 0.29 degrees with control on when excited by a random two-dimensional gust.

TABLE OF CONTENTS

LIST OF FIGURES

FIGURE

LIST OF SYMBOLS

α	Vane angle of attack (rad)
C_{Do}	Vane minimum drag coefficient
$C_{L\alpha}$	Vane lift curve slope (1/rad)
D	Drag of vane (lb)
E_I	Motor excitation or control voltage (volts)
E_{mp}	Voltage signal from motor potentiometer (volts)
E_s	Input voltage signal to amplifier (volts)
E_{wp}	Voltage signal from wing potentiometer (volts)
I	Vane moment of inertia including support arm (slug-ft^2)
I	Armature current (amp)
J_t	Total moment of inertia referred to the armature (lb-ft-sec^2)
K_b	Back-amp constant (v/rad/sec)
K_t	Torque sensitivity constant (lb-ft/amp)
ℓ	Moment arm of vane from pivot point to aerodynamic center of vane (ft)
L	Lift of vane (lb)
L_m	Armature inductance (hry)
m	Mass of vane (slug)
q	Dynamic pressure (lb-ft^2)
R_m	Armature resistance (ohms)
R_s	Equivalent source resistance (ohms)
S	Vane surface area (ft^2)
T_m	Motor torque (lb-ft)
U	Free stream velocity (ft/sec)

ζ	Vane damping ratio
ρ	Air density (slug/ft^3)
ρ_{vane}	Vane density (slug/ft^3)
θ	Pitch angle (rad)
τ	Torque (lb-ft)
ω	Angular velocity $\frac{d\theta}{dt}$ (rad/sec)
ω_n	Natural frequency (Hz)

ACKNOWLEDGEMENT

I wish to extend special thanks and appreciation to Mr. Stan Johnson for his assistance and technical expertise throughout the course of this thesis preparation. Also I wish to thank Professor Platzer whose guidance and comments were greatly appreciated.

I. INTRODUCTION

Practically at the outset of aviation history the alleviation of gust loads on aircraft was a concern to the aircraft designer. The development of larger, more flexible aircraft of greatly increased cost has considerably increased this concern. In addition, low level military operations and the anticipated increase in low level feeder and commuter routes indicate that effective methods for aircraft gust alleviation and flutter suppression might well pay large dividends in terms of lighter structures, larger payloads, more stable gunnery platforms, improved riding comfort and, perhaps most important, increased safety and extended service life.

One of the main arguments against an active gust alleviation system in the past has been the cost and complexity of such a system. This argument loses much of its impact in the light of present day realities when one considers that many existing aircraft cost in the neighborhood of 20 million dollars and have service lives of about 10 years. Any analysis of cost effectiveness would show that appreciable increases in service life could represent large savings in revenue over the life cycle of the aircraft. If larger payloads and increased crew efficiency are added, it is seen that the increased initial cost and complexity of an active load alleviation system may be worth serious consideration.

Perhaps the single most important thing that must be considered before incorporation of any load alleviation system is its reliability. Some insight into this problem can be gained when one considers that most present day aircraft already contain some type of stability

augmentation device. The advent of solid state electronics has made these devices extremely reliable. Thus, since any gust alleviation system would be built much along the lines of present day stability augmentation systems, it appears that one can already assume a high degree of reliability in-so-far as electronic circuitry is concerned.

In the final analysis any active load alleviation system, if it is to get aboard a production aircraft, must demonstrate an economic benefit and be extremely reliable.

A. PREVIOUS GUST ALLEVIATION STUDIES

Early attempts at gust alleviation were frequently devised without adequate analysis by their inventors. Nevertheless, they often achieved remarkable results. The wide variations in results was exceeded only by the innumerable and ingenious methods employed by their inventors.

Around 1930, Waterman (see Ref. 8 for more detailed review) devised an aircraft with skewed hinges attaching the wing to the fuselage. When lift forces overcame the force exerted by pneumatic struts the wing would deflect upward and rotate so as to reduce angle of attack in much the same manner as a rotor blade on a conventional helicopter. of course, the adverse effect of this arrangement on lateral control is obvious.

1. British Work

The British shortly after World War II designed a commercial aircraft to alleviate gust induced wing bending moments [Ref. 17]. Control was to be achieved through symmetrical deflection of ailerons in response to an input signal. While this aircraft was never placed in production, the system, with little preliminary analysis, was placed

aboard a Lancaster aircraft utilizing a vane gust detector with a hydraulically actuated control system. First engagement by the pilot resulted in a ride considerably more bumpy than without the system. By reversing the sign of the gain constant the ride was made somewhat smoother. The reason for this was that as the ailerons deflected up in response to an up gust an increased nose-up moment was produced which caused the aircraft to nose up even more due to the gust, thus offsetting the aircraft's natural tendency to relieve loads by nosing downward into an up gust. At higher frequencies the system actually did reduce some of the aircraft response to turbulence. However, at still higher frequencies (3 cycles per second) the system destabilized the wing first symmetrical bending mode.

2. Work of René Hirsch in France

By 1938, René Hirsch had completed a thesis on analysis and model tests of a gust alleviating airplane [Ref. 8]. As conventional servomechanisms were then in an early state of development, Hirsch relied on aerodynamic forces to actuate his system. He used forces on the horizontal tail to operate trailing edge flaps on the wing through a direct mechanical linkage. It may seem illogical to sense a gust aft of the place where its main effect will occur. However, as is well known, long-wavelength gusts have the greatest effect on aircraft response, and for this type of gust little change in phase effect results whether the gust is sensed at the nose or the tail of the aircraft. The recognition of this fact was one area in which Hirsch showed greater insight than most of his contemporaries

Hirsch conducted wind-tunnel tests of a dynamic model of his airplane. A venetian blind arrangement ahead of his model produced

the necessary gusts. Hirsch noted that with surfaces fixed his model would bang against the top of the tunnel under the influence of a gust whereas his alleviated model was relatively undisturbed. This type of dynamic testing of models was years ahead of its time and has since come into wide use for dynamic response testing.

Hirsch continued his work after World War II constructing a small clean twin-engine airplane equipped with his gust alleviation system. Hirsch's flap was actuated by the horizontal tail, which changed dihedral about chordwise hinges at the root. Hirsch's confidence in his design was so great that he designed the aircraft to a load factor of only 2 g, taking advantage of the weight saving to improve performance. His aircraft was well engineered and made many successful flights. The degree of alleviation he achieved was about 50% reduction in RMS acceleration values.

3. C-47 Test Results

A second experimental project with objectives similar to those on the British aircraft was conducted on a C-47 in 1952 [Ref. 10]. The ailerons were mechanically linked to the wing in such a manner that upward wing deflections would drive the ailerons upward. The mechanical linkage eliminated the need for incorporating a servomechanism and it was felt that this arrangement would be sufficiently reliable for use on service airplanes. Unfortunately this arrangement, in addition to suffering the same problems as the British aircraft, also had a tendency to flutter. This was due to the inertia of the ailerons, combined with the flexibility of the operating linkage, causing aileron deflection to lag wing deflection. This condition, being conducive to flutter, could only be eliminated if the gain between aileron deflection and

wing bending was left small. With this handicap the system was capable of only about 9 percent alleviation of wing bending moments, with no noticeable effect on riding comfort.

4. NACA Work

An exhaustive series of flight tests was conducted by NACA [Refs. 2,4,6,7,11] from 1952 to 1960 utilizing a small twin-engine transport. The tests were conducted in order to evaluate previous theoretical work and to demonstrate the feasibility of a gust alleviation system employing wing flaps and other control surfaces operated by a servomechanism. Provision was made for using either a nose-mounted vane or an accelerometer as the gust sensor.

A split elevator was used, the inboard section moving separately from the outboard section. The outboard section was connected to the flap through an adjustable linkage to balance the pitching moment. This section moved in phase with the flap. The inboard section was for pilot control.

The trailing edge flaps were also split into two sections in order to vary the downwash due to flap deflection. The small inboard section was used to change the flow field at the tail so as to reduce excessive pitching moments caused by flap movement in response to gusts. Each outboard flap section was connected to its aileron. Lateral control was achieved through differential movement while alleviation was accomplished using symmetrical control.

An electrohydraulic servomechanism was used to operate the flaps. In order to reduce the possibilities of structural wing feedback the flap servomechanism was designed to be highly attenuated at 8.0 cycles per second, the lowest natural frequency of the structure.

Power spectral methods were used in the analysis of flight test results. Vertical gust velocity was measured using vane angle of attack indications corrected for aircraft pitching and plunging motions. Test results showed that values of normal acceleration divided by gust angle of attack were about 50 percent smaller when the gust alleviation system was actuated. These results were somewhat less than expected. It was felt that flap response attenuation at high frequencies, and in particular an intentional velocity saturation characteristic which had been included as a safeguard against flutter, were largely responsible for this limitation. After the test results were analyzed, it was felt that a considerable improvement in alleviation performance could have been achieved by using a servo-mechanism with higher frequency response and more nearly linear characteristics.

5. Recent Work

Despite the success of earlier experiments there was little interest in the 1960's in incorporating a gust alleviation system aboard a production aircraft. One reason for this was that high speed aircraft with thin airfoil sections exhibited reduced structural frequencies. Thus there was the problem of providing adequate alleviation in the range of frequencies of interest to passenger comfort without exciting structural modes. Thus, active mode stabilization has become a topic of increasing interest and, in fact, for modern aircraft one needs to consider mode stabilization and gust alleviation together, if practical results are to be achieved, e.g., Refs. 1,3, 5,13,14,15,16,19,20.

Several theoretical works were published in the '60's; notable among these was a report published by the U. S. Army entitled "Gust

Alleviation Feasibility Study" [Ref. 20]. In this report, several alleviation systems, both active and passive, were studied. Among the systems investigated were vane controlled and accelerometer controlled systems as well as a novel telescoping wing concept. Effects of each system on items such as range, stability, structural effects, weight penalty and reliability were analytically investigated. While the results of this report are too lengthy to summarize, they make interesting reading for anyone involved in the design of gust alleviation systems.

Phillips, in reference 9A, goes into a detailed discussion of perhaps the two most common types of gust alleviation systems -- load sensing types wherein the gust loads on the wing are sensed by either strain gages or accelerometers; and vane types, wherein gust angle of attack is sensed. In this report he indicates that in the load sensing system the percent of alleviation increases with increasing speed, whereas in the vane type the percent alleviation tends to remain constant with speed as long as the gain is kept constant. He points out that one limitation of the load sensing type is the occurrence of a high frequency instability at a relative gain of one; that is, a gust inducing a load of plus one g on the sensor causes the gust alleviation system to respond with a negative one g response. He also points out that whereas the load sensing system is a closed loop system, the vane controlled system is more nearly an open loop system and thus, in the latter, the high frequency instability is much less likely to be encountered. This is so because operation of the angle of attack sensor causes deflection of the alleviation controls, but operation of the alleviation controls has only a minor effect on the indications of the angle of attack sensor.

Vane type systems are typically designed so that the effect of a uniform gust is completely counteracted by the alleviation controls. The main limitation of the vane system arises from the fact that sensing the gust at one point does not give a representative indication of the average angle of attack across the span. Alleviations as high as 80% may be obtained by using a single sensor mounted ahead of the nose to reduce accelerations.

Perhaps the most significant experimental work done in the late '60's was a major program involving the B-52. An Air Force sponsored program conducted by the Boeing Company and Minneapolis-Honeywell from 1964 to 1968 [Ref. 21] had the objective of developing a flight control and stability augmentation system that would provide improvements both in structural fatigue life and in rigid body and elastic mode stability in severe turbulence. Flight tests of the system as installed on a B-52H showed significant reductions in dynamic response to turbulence. Damping of the rigid body modes and low frequency antisymmetric aft-fuselage modes was increased. Lateral modes on the fin and aft fuselage were reduced more than 20% in turbulence. Fatigue damage rates were reduced more than 50% for these same locations. Test results agreed well with theoretical predictions. This system is now available in kit form for retrofit into the B-52G and H fleet.

In a later modification existing control surfaces including wing spoilers were used but actuators were modified in order to provide higher frequency response and symmetric deflection of ailerons. Flight test results indicated major reductions in fatigue damage rates and wing structural loads. The goal of 50% reduction in fatigue damage rates was achieved for all sensitive aircraft structures.

6. Present Work

Work presently underway at Langley Field, Virginia, by Boeing and NASA personnel is focusing again on a modified B-52 aeroelastic model fitted with modified aileron and flaperon and a nose mounted canard. The purpose of this work is to investigate the effect of active controls on structural damping as a means of preventing flutter and for use in gust alleviation. Initial results are encouraging and it is certain that the day when aircraft are designed with active control systems for flutter suppression and ride quality control is not far away.

Extensive work is also underway with the purpose of applying jet flap technology to the problem of relieving rotorcraft blade stresses. Reference 22 indicates that modulating the rotor loading by means of a multicyclic jet flap control system can reduce rotor blade stresses and vibratory loads transmitted to the fuselage.

II. SCOPE OF THIS RESEARCH

Rather than use conventional control surfaces as gust alleviators, as has mostly been done in the past, this thesis considers the use of a jet flap as the alleviator (Fig. 1).

A jet flap operates on the principle that air at high momentum is ejected from a spanwise slot at the trailing edge of the airfoil. This blowing at the trailing edge modifies the circulation around the airfoil and in fact may yield values of circulation greater than those attainable with boundary layer control. Two factors contribute to the increased lift on the jet flap. The direct component of jet momentum in the lift direction produces what is known as "reaction lift" and in addition the supercirculation creates a reduced static pressure on the upper surface and increases it on the lower surface. This effect is called "jet induced pressure lift". The total lift on the airfoil is the resultant of the basic airfoil lift plus jet induced pressure lift, plus reaction lift.

The first extensive tests on steady jet flap performance were conducted by Dimmock in 1956 [Ref. 24]. Other works by Stratford, Jacobs, and Spence [Refs. 25 and 26] did much toward refining steady jet flap theory. However, little theoretical knowledge exists regarding the oscillatory characteristics of jet flaps. For this reason, the jet flap gust alleviation system, which is the subject of this paper, had to be developed along experimental lines.

The jet flap used in this thesis is based on previous work by Simmons and Platzer [Ref. 12]. By varying the flow through two control tubes which impinge on the main stream either from above or

below, variable jet deflection angles are achieved (Fig. 1). It is then only necessary to sequence air flow to the two control jets in such a manner that lift effects due to gusts are cancelled by the lift due to the jet. This scheme would have particular appeal for aircraft STOL applications. The jet flapped configuration could provide the three functions of boundary layer control, conventional control, and gust alleviation, all with a single package. Other applications include the use of jet flaps on helicopter rotors to provide pitch and vibration control of the rotor.

Another factor which makes the jet flap appealing is the fact that the jet flap does not depend on the movement of a physical control surface having inertia. In fact, almost instantaneous deflection rates can be achieved. The only limitation in this regard seems to be the speed with which the control air can be sequenced.

It was decided at the outset to test the feasibility of such a jet flapped configuration by constructing a one degree of freedom wing model and testing its effectiveness in reducing torsional oscillations due to a sinusoidal gust field.

III. EXPERIMENTAL PROGRAM

A. MODEL CONSTRUCTION

A basic NACA 0010-66 airfoil section was chosen with a ten-inch chord and 14.15 inch span. The last 20% of chord was chopped off to allow installation of the main and control air tubes. Wing construction was of aluminum with conventional rib spar construction. Skin covering was of aluminum sheet with separate top and bottom panels to allow easy internal access for any required configuration modifications. Each end rib was constructed of 1/8" aluminum with a 3 1/2" cutout to allow insertion of a movable axle system (Fig.2) in order that pitch axis position could be varied. Next, two rectangular fittings were attached to the axle and inserted in the end rib cutout (Fig. 2). Screws through the top of each rib end held the axle firmly in place. Main and control air aluminum tubing was routed through the rectangular fitting. In order to eliminate the effect of these tubing connections on wing torsional response, tubing interfaces with the wing were made as nearly as possible to the axle position. The main air tube was routed through the left end rib and the two control tubes were routed through the right end rib. Plastic hose sections were used inside the wing to connect the air inlet tubes with the full span main and control tubes at the wing trailing edge. Plastic tubing was also used externally to the wing to supply main and control air for the wing.

Next, the wing with axle installed was mounted on bearings between two vertical supports. A horizontal arm soldered to the axle provided one attachment for a tension spring which was anchored to another arm

extending from the support (Fig. 3). This lower support could be adjusted so that various angle of attack positions could be achieved.

The basic wing and mounting problem was now complete. It should be noted that for the configuration to be statically stable in an air flow the elastic axis should be forward of the wing aerodynamic center. This position, however, left the wing with a very large tail heavy moment. This was easily corrected by adjusting the spring so that the tail heavy moment was cancelled out. Various springs were then tried until one was found which gave a reasonable value for natural frequency. It was found that a spring with a constant K = 2.5 lb/in gave a natural frequency around 2.45 Hz. This spring was deemed acceptable and used for all subsequent tests.

B. VANE DESIGN

Model construction now completed, it was necessary to select a sensor to detect gust angle. The two most common types for gust measurement were found to be a simple vane arrangement mounted ahead of the wing or an accelerometer mounted on the wing. The vane sensor was selected primarily because it was felt that this would allow greater flexibility in that vane position could be easily varied in order to account for lags in time between the gust striking the vane and striking the wing. Appendix A shows that, for a simple vane, the natural frequency and damping ratio are given by

$$\omega_n = U \left(\frac{(C_{L\alpha} + C_{Dmin}) S \rho \ell}{2I} \right)^{1/2}$$

$$\zeta = \omega \frac{\ell}{2U}$$

It may be noted that the natural frequency depends upon surface area, length and inertia, all functions of vane size and weight. In general, when any one of these change, the others change also so that a specific vane to give a specified value of natural frequency and damping factor would require an iteration process. This was done by means of a simple computer program wherein the various parameters were sequentially varied with ζ and ω_n calculated at each step. Not surprisingly, the results indicated that for a high natural frequency and damping ratio near 0.7, the vane should be as light and as small as possible. Since the vane was to drive a low torque potentiometer it was decided that, in order to be able to neglect this small amount of friction, the vane should probably have at least a 4" pivot arm. The final vane chosen is shown in Fig. 4. The theoretical values for ζ and ω_n were found to be

$$\zeta = 0.55$$

$$\omega_n = 13.75 \text{ Hz}$$

for a tunnel velocity of 31 ft/sec. This was the maximum velocity attainable in the low speed smoke tunnel where testing was to be conducted. It should be noted that the vane was mounted on its own support independent of the wing. Thus it was not necessary to subtract out wing motion in order to obtain true gust angle of attack, as would be the case if the vane were attached to the wing. Subsequent experimental tests of the vane showed that at 31 ft/sec the vane had a damping ratio of 0.58 and a natural frequency of 11.37 Hz thus showing good agreement with theory.

C. CONTROLLER

A D.C. torque motor, designation T-2171, made by Inland Motor Company, was used to control air being routed to the jet flap. Specifications for this motor are listed in Appendix B.

The basic torque motor was fitted with a pancake mounted tachometer, Inland Motor Company designation TG-2123-D, and a rotary potentiometer, both for motor stabilization purposes. Tachometer characteristics are listed in Appendix B. Necessary amplification was provided using a MODEL 150A Hyband DC Servo Amplifier. Specifications for this amplifier are also listed in Appendix B.

A detailed analysis to obtain the controller transfer function was carried out in Appendix C. It was found that this analysis was of limited value, however, due to the presence of a pneumatic valve which introduced highly non-linear effects into the system which could not be readily analyzed. In order to more firmly define controller response, a frequency response was made. This test was made with the motor connected to a 4-way pneumatic valve as shown in Figure 5. Air pressure through the valve for this work was a nominal 13 PSIG. Results of the frequency response run are shown in Figure 6. It was found from this test that a "jump" phenomena occurred at 17 cy/sec confirming the non-linear nature of the controller. This fact however was of little concern due to the fact that the system was quite linear up to frequencies of about 11 cy/sec. Since, as will be shown later, wing response to frequencies above 6 cy/sec was negligible, a good experimental curve fit was found to be

$$\frac{E_{mp}}{E_s} = \frac{1}{1 + .005s}$$

where E_{mp} is the motor potentiometer voltage and E_s is the input signal

voltage. This approximate curve fit is shown in Figure 6 and agrees closely with experimental results below 11 cy/sec.

D. AIRSTREAM OSCILLATOR

The method used to obtain the required gust field was to use a rigidly mounted jet flap. By mechanically deflecting the jet either an upwash or downwash field could be generated. The method of deflecting the jet was to rotate the main tube by means of a motor bell crank mechanism (see Figure 7). The main tube was similar in construction to that used on the model under investigation except that on the oscillator the tube was moveable while on the model it was fixed. The deflection angle at the trailing edge could be oscillated through angles of ± 20° at tunnel speeds up to 31 ft/sec and frequencies up to 10 cy/sec.

Originally it was intended to mount the vane and wing ownstream of the oscillator in the following manner.

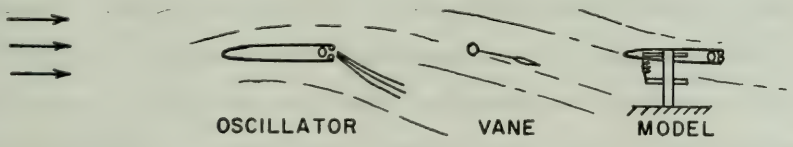

In this manner, the vane would sense the gust and signal the controller, which would then route air to offset the gust as it approaches the wing. However, this approach was abandoned initially due to the fact that random turbulence generated by the oscillator housing superimposed random frequencies on the basic sine wave. It was felt that this

situation should be avoided initially until the gust alleviation system could be made to function in the presence of a purely sinusoidal gust.

The model was then placed just upstream of the oscillator and under the action of the oscillator was found to undergo purely sinusoidal oscillation in torsion at a frequency governed by the oscillator. In this position, however, it was found that if the vane were placed further upstream, it would sense the upwash of the model rather than the oscillator. At this juncture it was decided to abandon for the moment the original idea of having the vane upstream of the model, and to settle upon a vane location where it would sense oscillator gusts with minimum turbulence distortion. It was realized that this approach would only be valid for a sinusoidal gust of constant frequency and amplitude and that any random gusts would have already influenced the wing before actually being detected by the vane. However, as long as the gust was a steady sinusoid the phasing differences between vane and model could be accounted for by a phase shifter in the control system. Actual arrangement of the vane, wing, and oscillator is shown in Figure 8. Hereafter, this arrangement shall be referred to as configuration A, while the vane ahead configuration will be referred to as configuration B. Appendix D summarizes properties of the flow field produced by the oscillator.

E. WIND TUNNEL

The Low Speed Flow Visualization Facility at the Naval Postgraduate School is essentially a three-dimensional open circuit smoke tunnel. The air inlet is a square bell shaped configuration containing a honeycomb three inches thick followed by one layer of screen. The inlet

area is 15' x 15' and subsequently contracts to a 5' x 5' x 12' square test section.

The air flowing through the test section passes through a set of louvers downstream of the section and transitions from a square to a circular cross section. Behind the louvers in the circular cross section is a fan that controls the air flow through the tunnel. Between the louvers and the fan is a rubber sleeve to prevent the motor vibrations from being transmitted into the test section. The fan is driven by a motor mounted directly behind it. The air after passing through the fan is turned vertically upward and vented to the atmosphere outside the building. Maximum tunnel speed is 32 feet/second.

F. OPEN LOOP VANE CONTROLLED SYSTEM

The open loop control system is shown in Figure 9. It can be seen that a gust signal sensed by the vane was converted to an electrical signal by means of a high precision low torque rotary potentiometer. This signal was then routed to a phase shifter. The phase shifter was actually a band pass filter which, in addition to allowing a wide range of phase angles, also provided some signal shaping of the vane signal, which was found to contain some higher frequencies due to its close proximity to the oscillator.

After signal shaping and phase shifting, the signal was routed to the controller which consisted of the amplifier, torque-motor, tachometer, and motor-mounted potentiometer for position feedback information. It should be noted that the rate and position feedback provided by the tachometer and potentiometer do not make the system as a whole closed loop since they act merely to improve controller response and no direct wing feedback is incorporated. The electrical signal which entered

the controller is converted to a shaft angle by the servomotor. This angular rotation is converted to linear motion by the mechanical linkage shown in Figure 5. The semicircular arrangement shown atop the motor shaft was for mass balancing of the load applied to the shaft. The pneumatic valve had one inlet and two outlets for central air to be routed to the wing. This valve metered air at 13 PSIG to one control tube or the other depending on whether motor shaft angle was positive or negative. For zero motor shaft angle, no air was routed to the control tubes.

Air metering was approximately proportional to shaft angle position rather than being of a "flip flop" nature. This allowed smooth control of air to the appropriate control tube. When this air was expelled from the control tube at the model, momentum interaction with the main jet sheet (at 68 PSIG) allowed variations in jet blowing angle over a range of 10 degrees. Thus model motion in torsion was achieved by varying jet deflection angle.

It was anticipated that model response (in one-degree-of-freedom torsional motion) to controller input would be of a second order nature. An experimental frequency response test at frequencies from 0.2 - 4.6 cy/sec was carried out to verify this. The results in Figure 10 indicate that indeed the gain of $\frac{\text{wing position}}{\text{motor position}}$ was of second order. However, the phase angle variation did not have the classical second order variation. That is, at resonance, instead of the expected phase angle of -90°, the phase angle was -119°. In fact, the phase angle showed a linearly increasing gain over expected second order values.

Further investigation revealed that fixed time delays within the air tubes leading from controller to model were responsible for this

phasing error. This time delay was found to be approximately 0.04 seconds. The actual transfer function for a pure time delay is $e^{-\tau s}$ where τ is the value of the time delay. A first order approximation of this time delay, that is $\frac{1}{1 + \tau s}$, was found to give good correlation with experimental results. The resulting transfer function for the wing plus fixed transport delays was found to be

$$\frac{E_{wp}}{E_{mp}} = \frac{28}{(S^2 + 3.696S + 237.16)} \left(\frac{1}{1 + .04S}\right)$$

where the second term represents the transport delays. From this equation it was found that for the oscillating wing

$$\zeta = 0.12 \quad \text{and} \quad \omega_n = 2.45 \text{ Hz.}$$

IV. TEST PROGRAM AND RESULTS

A. CONFIGURATION A TESTING

With all elements positioned and wing elastic axis set at 30% chord, the tunnel was turned on. The oscillator was then turned on and the sinusoidal gust frequency adjusted to 2.45 Hz, the natural frequency of the model. In this condition the wing oscillations were roughly equal to 3° about level position. Next the automatic control functions were powered and a decrease in wing oscillations was immediately noticed. By adjustment of the high and low cutoff frequencies of the band pass filter, the phase shift of the vane relative to the model was slowly varied until model oscillation was hardly perceptible. In this position the low and high cutoff frequencies of the filter were 0.6 Hz and 20 Hz respectively. A strip chart recording of wing angular position similar to Figure 11 showed that wing torsional oscillations had been reduced by 92%.

Greatly encouraged by this early success, parameter variation studies were next conducted. Control system pressure was varied about the optimum value of 13 psi. Alleviation seemed to fall off rather linearly as control pressure was reduced. However, with an increase in pressure of three or four psi, alleviation was observed to rapidly deteriorate. It was felt that this was probably caused by a sudden wall attachment commonly known as the "Coanda Effect". This sudden attachment had the effect of causing the system to operate in a "bang-bang" fashion rather than proportionately, as originally designed.

Main air pressure was not varied from its nominal value of 68 psig due to the fact that oscillator air pressure was also fed from the same

compressor and the 68 psig was needed by the oscillator if adequate wing motion was to exist.

Gain variations were then made about optimum and it was noted that alleviation degradation was approximately linear with gain reductions. Gain increases were not investigated as servo motor operation was already very near the pneumatic valve stops.

Band pass filter variations from the 0.6 Hz and 20 Hz values seemed to affect alleviation ability only slightly with small variations from optimum. In fact, increasing the high cutoff frequency from 20 to 200 Hz reduced alleviation only a few percent.

One factor discovered by accident had considerable effect on alleviation ability. This was servo-motor reference, or neutral position. If this reference were varied a slight amount from the neutral position the wing would merely assume a new angle of attack with no loss of alleviation capability. However, large changes in this reference position caused rapid loss in alleviation. Again, this sudden loss was caused by the Coanda Effect, wherein the jet flow was attaching to one of the control tubes, causing a sudden large incremental jet deflection angle. As long as the motor reference position was reasonably centered, however, this effect caused no major problems. One cure for the above problem would be to make the control tubes flatter, with sharp trailing edges. In this manner, flow attachment would not occur.

After completion of the parameter variation studies already discussed, it was decided to encase the wing between two fixed sideplates to provide a two-dimensional flow field before further study of the system was carried out. This reconfiguration was carried out with a 0.1-inch gap between each wing tip and its endplate. It was felt that this gap

would be sufficient to allow the model enough clearance to oscillate while still providing an essentially two-dimensional flow field. One factor that complicated sidewall construction was the need to provide holes in the sidewalls just sufficient for the oscillating axle and tube assembly to pass through, yet small enough to maintain essentially two-dimensional flow. This problem alone consumed considerable time in alignment and rework. Sidewall height was 26 3/4" and base was 22 3/4". The sidewalls, one of 1/4-inch aluminum and one of 3/8-inch plexiglass (to permit viewing) were attached to a wooden base below. A crossmember on top provided horizontal separation and rigidity between the sideplates. When installed, an unexpected Venturi effect around the wing tended to pull the sideplates inward, causing rubbing with the oscillating wing. Tension cables with adjustable turnbuckles were installed to alleviate this problem. However, these required frequent adjustment so that exact uniformity in test conditions from day to day was a virtual impossibility. In fact, slight variations in endplate gap exhibited such a marked influence on wing damping coefficients that in one test the wing was found to exhibit neutral dynamic stability when given a slight angle of attack. When sidewall gap was increased by only 1/32 of an inch, the wing was then found to have a damping value of 0.2 times critical. This marked change in wing damping could not be explained and requires further study. A large series of tests run on many different days showed that wing damping values generally seemed to vary between 0.1 and 0.2 times critical.

On reflection it was felt that a much better method for obtaining two-dimensionality would have been to attach endplates rigidly to the wing, thus eliminating all gap and leakage problems at the outset. This approach, though considered, was not adopted because it was felt that the

decrease in bandwidth which would result from the increase in model inertia would prove to be too large. The model bandwidth was only 3.74 Hz without sidewalls and to reduce this would have seriously limited testing flexibility since the lowest sinusoidal gust which the oscillator could develop was around 1.7 Hz. Perhaps the added material could have been light and rigid enough so that bandwidth reduction would be minimal.

Any future studies should certainly give serious consideration to this latter alternative. Nevertheless, despite the limitations already discussed, the model as modified did prove to be an acceptable testbed for further studies of the gust alleviation system.

After the system was again assembled and checked out, testing was resumed. At a tunnel speed of 31 feet/second, gust frequency was varied from 2.2 to 3.8 Hz. At each frequency, wing osciallations were measured first with control air off, then with control air on. Figure 12 shows the results of this study which clearly illustrates the effectiveness of the system in alleviating sinusoidal gusts. It may be noted that with control off the wing oscillations vary from ±3.4° at 2.25 Hz to about ±0.85° at 3.62 Hz, while with control on the oscillations remain fairly constant at ±0.5°, regardless of frequency. Figure 13 shows percentage alleviation versus frequency. The falloff in percentage alleviation with increasing frequency is perhaps misleading. It is due more to the fact that wing response at the higher frequencies was so low that it fell within the noise levels of the control system. In this region response either to turbulence or control actuation was very small.

While it would seem intuitively that zero wing deflection angles should be attainable for a sinusoidal gust with control on, this result was not possible for the system as assembled due to the fact that while

the wing was undergoing pure sinusoidal motion, the vane mounted downstream in close proximity to the oscillator was undergoing oscillations as shown below.

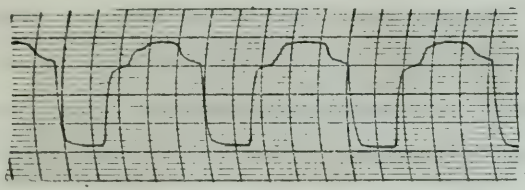

Even though filtering removed most of the harmonics from the signal, it was felt that the amount of variation which remained along with other slight system nonlinearities was sufficient to account for the deviations from perfect 100% gust alleviation.

Next, tunnel velocity was varied with the wing exposed to a constant sinusoidal gust field of ω = 2.25 Hz. Figure 14 shows that alleviation remains fairly constant down to a velocity of 17.5 feet/second, after which it drops off drastically. If accurate, this result would seriously limit the applicability of this type of system, however, several points deserve mention. As tunnel velocity was reduced, gust upwash velocity remained the same, thus the gust angle of attack was greatly increased as tunnel velocity was reduced.

Since in the optimum operating condition at ω = 2.25 Hz and V = 31 feet/second the controller was operating near full authority, there was little additional control force which could be brought to bear on this apparently increased gust. Additionally, at the lower velocities the vane located beneath the oscillator was receiving extremely large input signals, causing the pneumatic valve to be driven into its mechanical stops. Thus the system was saturated and no longer able to operate in its linear range. For this reason, as indicated in Figure 14, the gain

of the vane signal was reduced about 20% below 17 feet/second in order to prevent this saturation. Of course, the effect of this limited authority on alleviation capability is apparent below 17 feet/second. It should be realized that in a conventional vane-ahead configuration (Configuration B, to be considered later in this report) this saturation effect would not occur. The alleviation system would be designed such that full authority control actuation is sufficient to counteract some specific maximum expected gust within the flight speed envelope. The only effect which would occur would be a slight falloff in alleviation capability as airspeed was varied about some design value. This is so because at the design speed the time lead of the sensor, i.e., the time between when the gust strikes the vane and when it strikes the wing, is equal to the time lags within the system, i.e., transport lags and any frequency sensitive lags introduced by the servo-motor. At any faster speed (for fixed vane location) the time lead from the vane is lessened, thus time lead and lag are no longer equal and alleviation is no longer optimum. This problem could easily be remedied by providing electronic lead or lag circuitry.

B. CONFIGURATION B TESTING

Having had considerable success with configuration A, it was decided to rearrange the system components so that the oscillator was now upstream, followed by the vane at about two feet behind the oscillator trailing edge. Based on system time delays of 0.04 seconds, the model was placed (.04 sec) x (31 ft/sec) or 1.24 feet behind the vane aerodynamic center. As arranged, and with the wing elastic axis at 30% chord as before, it was found that wing oscillations even with control off were insufficient to record. In an effort to increase the amplitude of

oscillation, the wing pitch axis was shifted to 44% chord. In this position, as expected, the wing was slightly statically unstable due to the fact that the pitch axis was aft of the aerodynamic center. However with tunnel air on, the wing would merely seek a new reference at about ±1° angle of attack. While not a stable equilibrium point with the oscillator turned on, the wing did undergo sinusoidal oscillations about the zero angle of attack position with amplitudes of nearly ±2°. In this configuration, it should be noted that both the oscillator and main air tube were set at 33 psi while the control tube pressures were reduced to 7 psi. These pressures seemed to provide more sinusoidal gusts than the 65 psi used in configuration A.

Initial application of servo power was found to yield negligible controller response. Therefore, the amplifier gain was increased in order to account for the reduced gust signal input being sensed by the vane in its new position. Subsequent investigation showed that the gust oscillator was able to generate a gust amplitude of ±5° at the nominal tunnel speed of 31 feet/second. With the increase in gain control, system effectiveness was again found to be excellent in reducing sinusoidal oscillations.

It was decided to remove the band pass filter in order to simplify system complexity as much as possible. When this was done, no noticeable change in system performance was observed so that all configuration B testing was done without the filter.

It was felt that without the filter the frequency response of the system should be better at the higher frequencies. Figure 15 clearly shows this to be the case. In fact above 3 Hz configuration B was more than twice as effective as configuration A and the system was effective up to about 6 Hz, whereas configuration A was only effective to about 4 Hz.

This result was deemed most gratifying since configuration B with the vane sensing the oncoming gust upstream of the wing was much more closely related to actual flight conditions than configuration A.

Figure 16 shows wing deflection angle versus frequency. Again the falloff in wing response with frequency is noted for the case of no control, whereas with active control applied wing response is almost constant.

In order to further measure system performance wing rotation angle was fed into a spectrum analyzer. Figure 17 shows the power spectral density, system off, then on, when subject to a constant amplitude sinusoidal gust at 3.25 Hz. It should be noted that, at the forcing frequency, the wing signal squared is 30 db less with active control applied. It may also be noted from Figure 17(b) that the wing response at the forcing frequence is only slightly above the surrounding level of noise.

As promising as the system appeared, it was realized that aircraft in turbulence seldom encounter sinusoidal gusts at constant frequency. A method for generating random gusts needed to be devised if the system was to be rigorously tested.

One method considered was to drive the oscillator with a servo motor similar to the one used to operate the pneumatic valve. The motor could be directly linked to the oscillator main control tube and, as the tube had little inertia, high rotation rates could be achieved (to approximately 17 Hz for this particular motor). A Gaussian noise generator could then be used as input to the servo motor to produce a pure white noise type of turbulence or could have been fed to the motor via a filter constructed so as to duplicate any atmospheric turbulence model desired. To this writer's knowledge, no such tool presently exists and such a device would certainly prove beneficial to the study of wind tunnel models in turbulence. As appealing as this idea was, time and material

limitations precluded the installation of such a random gust generator. Nevertheless, by uncoupling the main air tube of the oscillator from the motor drive mechanism it was possible to rotate the main tube manually. A mechanical linkage through the tunnel floor enabled an operator below to mechanically introduce a two-dimensional gust with "random" content limited only by the randomness of the operator's hand motion.

Figure 18 shows a time history of wing and vane motion with control off then on. The reduction in wing motion is readily apparent with control on. It may be noted that wing response with control on never exceeds 0.9° during this six-second run, while without control this level is exceeded seven times.

V. SUMMARY AND RECOMMENDATIONS

This thesis investigated the feasibility of using a jet flap in a gust alleviation role. A vane gust sensor provided the signal for servo motor actuation of a pneumatic valve which controlled the sequencing of air to the trailing edge of the airfoil. Under the action of a steady sinusoidal gust the control system was found capable of alleviating 92% of the pitching motion due to the gust. Additionally, analysis of the time history shown in Figure 18 due to a random gust indicated that without alleviation the wing RMS level was 0.68° while with control on this level was 0.29° corresponding to a percentage reduction in RMS signal level of 57%.

It was felt that this result sufficiently demonstrated the feasibility of the system investigated. Of course it is realized that the step from simplified model to full scale aircraft is a large one. Future studies should perhaps be directed toward the construction of a model equipped with jet flaps so that both pitching and plunging modes can be acted upon simultaneously. Elevator to wing control surface gains would have to be worked out so that the moment imbalance created by an approaching gust would be offset by the elevator motion. In addition, wing control-surface-to-vane angle gains would need to be found so that aircraft translation was minimized.

Unfortunately, much of this work would have to be done by trial and error as there are still a great many gaps in oscillatory jet flap theory. Nevertheless, it is work which must be done if a jet-flapped gust alleviation is to ever be seriously considered for installation on a production aircraft.

APPENDIX A - VANE DESIGN

To be effective as a gust detector a vane must have the best possible response characteristics with as high a natural frequency as possible. An analysis similar to that carried out by D. Graham [Ref. 23] was carried out assuming a statically balanced vane as shown in Figure 1.

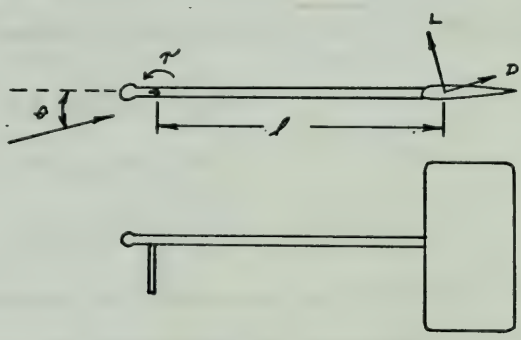

Additionally it was assumed that potentiometer bearing moment was negligible compared to that developed by the vane. The equation of motion for this system can be written as

$$\ddot{\theta} + 2\zeta\omega_n\dot{\theta} + \omega_n^2\theta = 0$$

with the two quantities ζ and ω_n the system parameters one seeks.

The torque tending to rotate the vane to zero angle θ is,

$$\tau = (L \cos\theta + D \sin\theta)\,\ell \qquad (1)$$

Here L and D are the lift and drag components on the vane and is the moment arm from the axis of rotation of the vane. For small angles

$$\cos\theta \simeq 1 \text{ and } \sin\theta \simeq \theta$$

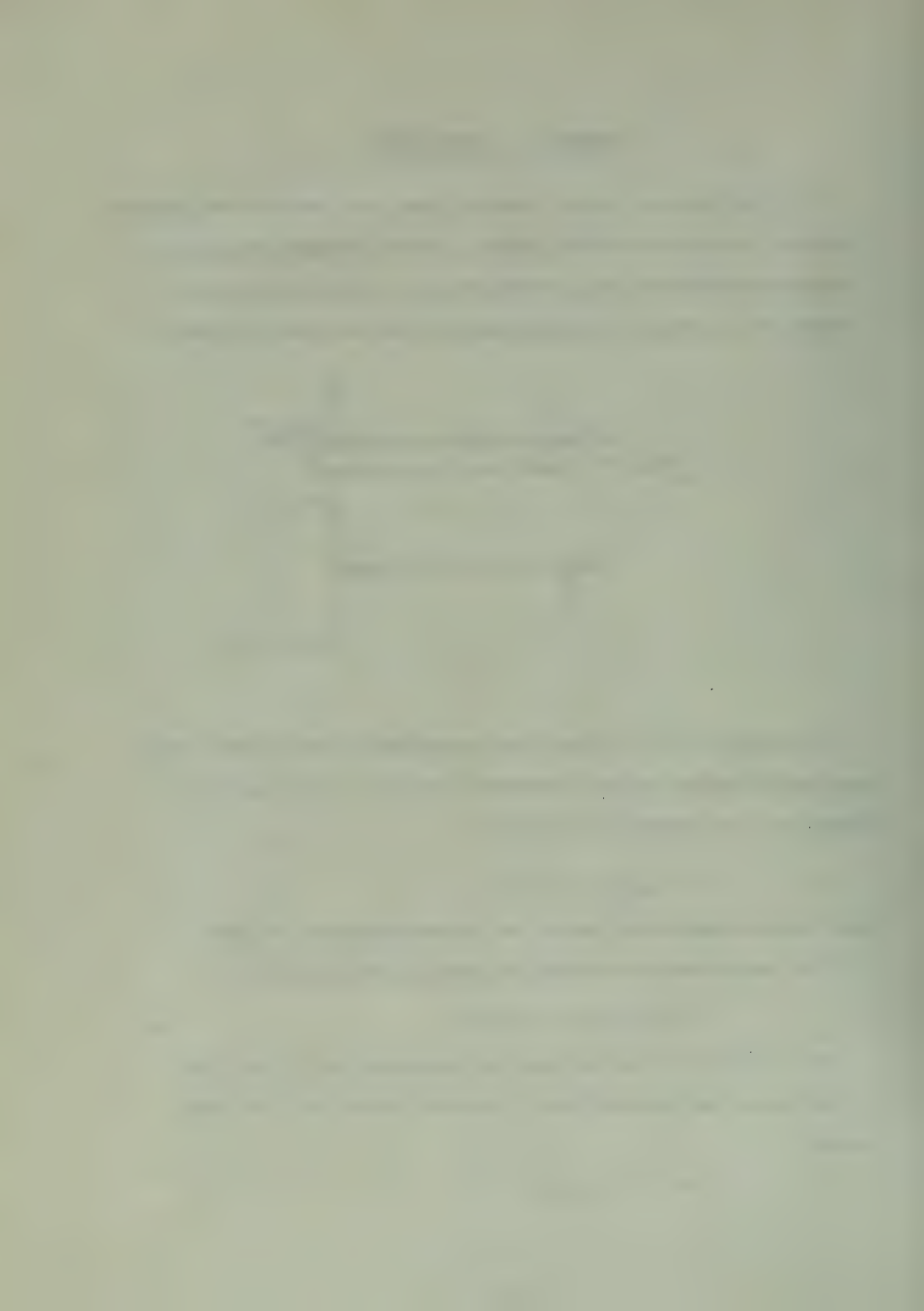

or

$$\tau = (L + D\theta)\,\ell \tag{2}$$

Incorporating the definition of lift curve slope and drag curve slope, i.e.

$$L = (\frac{dC_L}{d\alpha})\alpha Sq = (\frac{dC_L}{d\alpha})\theta Sq \tag{3}$$

$$D = [(\frac{dC_D}{d\alpha})\alpha + C_{Do}]Sq = [(\frac{dC_D}{d\alpha})\theta + C_{Do}]Sq \tag{4}$$

where C_{Do} is the parasite drag coefficient, S is the vane area and q is the dynamic pressure. Substituting (3) and (4) into (2) results in

$$\tau = [(\frac{dC_L}{d\alpha})\theta + (\frac{dC_D}{d\alpha})\theta^2 + C_{Do}\theta]Sq\ell$$

differentiating with respect to θ

$$\frac{d\tau}{d\theta} = [(\frac{dC_L}{d\alpha}) + 2(\frac{dC_D}{d\alpha})\theta + C_{Do}]Sq\ell$$

where $\frac{d\tau}{d\theta}\theta$ represents the torque due to vane deflection. Additionally, the torque due to vane velocity must be considered. These torques arise from changes in vane angle of attack due to angular velocity. For small angles this change in angle of attack will be

$$\Delta\alpha = \frac{\dot{\theta}\ell}{U}$$

In the presence of a pitching rate, the θ in (2) becomes $\theta + \frac{\dot{\theta}\ell}{U}$. With these substitutions the torque can be written

$$\tau = [(\frac{dC_L}{d\alpha})\frac{\dot{\theta}\ell}{U} + (\frac{dC_D}{d\alpha})\frac{\dot{\theta}\ell}{U}(\theta + \frac{\dot{\theta}\ell}{U}) + C_{Do}(\theta + \frac{\dot{\theta}\ell}{U})]Sq\ell$$

differentiating with respect to $\dot{\theta}$

$$\frac{d\tau}{d\dot{\theta}} = [(\frac{dC_L}{d\alpha})\frac{1}{U} + \frac{dC_D}{d\alpha}(\frac{U\theta + 2\dot{\theta}\ell}{U^2}) + \frac{C_D}{U}]Sq\ell^2$$

The equation of motion

$$I\ddot{\theta} + \frac{d\tau}{d\dot{\theta}}\dot{\theta} + \frac{d\tau}{d\theta}\theta = 0 \tag{5}$$

can now be written.

$$I\ddot{\theta} + [(\frac{dC_L}{d\alpha})\frac{1}{U} + \frac{dC_D}{d\alpha}(\frac{U\theta + 2\dot{\theta}\ell}{U^2}) + \frac{C_D}{U}]Sq\ell^2\dot{\theta}$$
$$+ [(\frac{dC_L}{d\alpha}) + 2(\frac{dC_D}{d\alpha})\theta + C_{Do}]Sq\ell\theta = 0 \qquad (6)$$

Since $\frac{dC_D}{d\alpha}$ is small with respect to $\frac{dC_L}{d\alpha}$ for small angles of attack this term is dropped, yielding:

$$\ddot{\theta} + [(\frac{dC_L}{d\alpha}) + C_{Do}]\frac{qS\ell^2}{UI}\dot{\theta} + [(\frac{dC_L}{d\alpha}) + C_{Do}]\frac{qS\ell}{I}\theta = 0 \qquad (7)$$

Since this equation is of the form

$$\ddot{\theta} + 2\zeta\omega_n\dot{\theta} + \omega_n^2\theta = 0$$

$$\omega_n = \frac{(C_{L\alpha} + C_{Do})Sq\ell}{I} = U\frac{(C_{L\alpha} + C_{Do})S\rho\ell}{2I} \qquad (8)$$

$$\zeta = \frac{1}{2\omega_n}[(C_{L\alpha} + C_{Do})\frac{qS\ell^2}{UI}] = \frac{1}{2\omega_n}(\frac{\omega_n^2\ell}{U}) = \frac{\omega_n\ell}{2U}$$

or substituting for ω_n,

$$\zeta = \frac{(C_{L\alpha} + C_{Dmin})S\rho\ell^3}{8I} \qquad (9)$$

Equations (8) and (9) show the dependence of natural frequency and damping ratio on vane characteristics. As one can readily see, no simple method for predicting vane size for some high value of ω_n is apparent.

If, however, the inertia of the vane arm is neglected, as well as the moment of inertia of the vane platform about its CG, it can be seen that

$$I = m\ell^2 \quad \text{and} \quad m = \rho_{vane}(St)\ell^2$$

where t is the vane airfoil thickness.

Then one can write:

$$\omega_n = \frac{(C_{L\alpha} + C_{Do})Sq\ell}{\rho_{vane}\, St\ell^2} \quad \text{or} \quad \omega_n \propto 1/\sqrt{\ell}$$

Thus, the smaller the value of ℓ, the higher the natural frequency.

APPENDIX B

T-2171-C D.C. TORQUE MOTOR SPECIFICATIONS

Peak torque at stall (25°C)	0.63 lb-ft
Peak power at stall (25°C)	50 watts
Continuous torque at stall (25°C)	0.34 lb-ft
Continuous power at stall	14.8 watts
No load speed	57 rad/sec
Damping factor	0.012 lb-ft/rad/sec
Electrical time constant	1.5 msec
Friction	0.016 lb-ft
Rotor inertia	9.9×10^{-5} lb-ft-sec^2
Maximum shaft power	12 watts
Maximum power rate	3958 lb-ft/sec^2
Motor Constant	0.089 lb-ft/watt$^{1/2}$

DIMENSIONS

Outside Diameter	2.81 in
Inside Diameter	1.00 in
Thickness	1.50 in
Weight	25 oz

WINDING CONSTANTS

D.C. resistance (25°C)	6.7 ohms
Volts at peak torque	18.1 volts
Amps at peak torque	2.7 amps
Torque sensitivity	44.9 oz-in/amp
Back EMF	0.32 volts/rad/sec
Inductance	10 mhry

TG-2123-D TACHOMETER GENERATOR SPECIFICATIONS

Friction torque	1.2 oz-in
Rotor inertia	0.007 oz-in-sec^2
Weight	9 oz

WINDING CONSTANTS

D.C. resistance	100 ohms
Voltage sensitivity	0.040 volts/rad/sec
Inductance	0.057 hrys
Minimum load resistance	10 K ohms
Maximum operating speed	40 rad/sec
Voltage at maximum operating speed	16.0

HYPAND 150A D.C. SERVO AMPLIFIER SPECIFICATIONS

Output power	150 watts nominal
Output voltage (minimum) (B+ at 28 VDC)	±22 VDC
Output current (Adjustable limit)	±7 amp
Current limit temperature drift	+0.2%/deg C maximum
Output impedance	0.2 ohms
Maximum non-destructive signal input voltage	±100 volts
Input impedance	75 M ohm
Input power	+28 VDC±10%, 75 amps max.
Quiescent current (maximum)	100 ma
Load resistance (minimum)	0 ohm
Preamp gain (open loop)	50,000 volts/volt
Preamp drift (voltage referred to input)	<10μv/°C

Power stage gain	10 v/v±20% at 25°C
Power stage drift (referred to input)	<200 μv/°C
Power stage dead band (referred to input)	<±20 mv at 25°C

APPENDIX C - TRANSFER FUNCTION DERIVATION FOR CONTROLLER

Considering first the motor alone and assuming negligible friction and load torque, the expression between developed torque and current can be written:

$$T_M = K_T I = J_T \frac{d^2\theta_o}{dt^2} \tag{1}$$

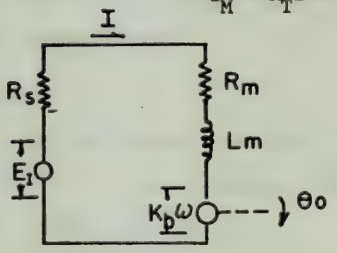

Equivalent Circuit for Motor

Next, voltages are summed around the equivalent circuit above.

$$E_I = I(R_M + R_S) + L_M \frac{dI}{dt} + K_B \frac{d\theta_o}{dt} \tag{2}$$

Now take the Laplace transform assuming zero initial conditions.

$$E_I = (R_M + R_S)I = L_M IS + K_B \theta_o S \tag{3}$$

Equation (1) becomes,

$$K_T I = J_T \theta_o S^2 \tag{4}$$

Combining (3) and (4) to eliminate I

$$\frac{\theta_o}{E_I} = \frac{1}{S\left(\frac{LJ_T}{K_T} S^2 + \frac{JR}{K_T} S + K_B\right)} \quad \text{where } R = R_M + R_S \tag{5}$$

The following values were used in (5) above:

$J_T = 1.7 \times 10^{-4}$ slug-ft^2 $\qquad K_B = 0.32$ v/rad/sec

$K_T = .234 \frac{\text{lbf-ft}}{\text{amp}}$ $\qquad R_T = 7$ ohm

$L_M = 0.01$ hry

When substituted into (5) we obtain

$$\frac{\theta_o}{E_I} = \frac{1}{S^3(7.26 \times 10^{-6}) + S^2(.00509) + S(.32)} \tag{6}$$

Neglecting the cubic term (6) becomes after simplifying

$$\frac{\theta_o}{E_I} = \frac{3.125}{S(.0159S + 1)} \tag{7}$$

This is the transfer function for the motor acting alone with no compensation.

The tachometer transfer function is found in the following manner:

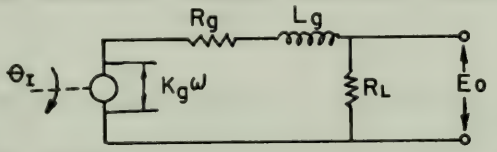

Equivalent circuit for tachometer

Writing the loop equation for the equivalent circuit above,

$$K_g \theta_i S = (R_g + R_L) I_g + L_g I_g S \tag{8}$$

$$E_o = I_g R_L \tag{9}$$

Combining (8) and (9) to eliminate I_g

$$\frac{E_o}{\theta_i}(S) = \frac{K_g S}{(\frac{R_g}{R_L} + 1)(1 + \frac{L_g S}{R_g + R_L})}$$

Using the following values

R_L = 2000 ohm $\qquad$ K_g = 0.4 v/rad/sec

R_g = 100 ohm $\qquad$ L_g = 0.057 hry

then

$$\frac{E_o}{\theta_i}(S) = .381\ S$$

Having the transfer functions for motor and tachometer, the transfer function for the entire controller can now be formed.

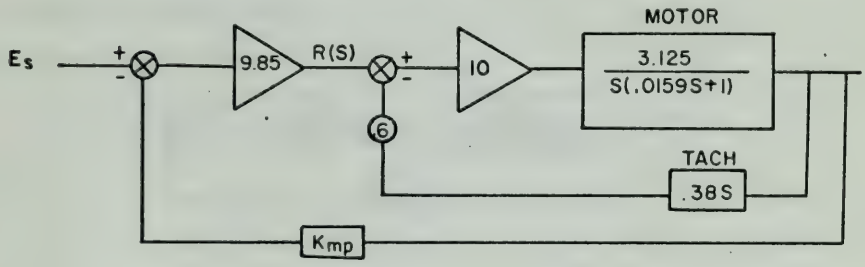

The above figure indicates the additional components in the controller. The values shown were found to give good controller response. From control theory it is known that for a system similar to that shown below,

$$\frac{E_o}{E_i} = \frac{G(S)}{1 + G(S)H(S)} \qquad (11)$$

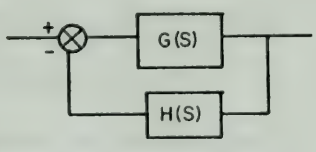

If only the inner loop of the controller is considered a simplified block diagram results from which an intermediate transfer function results.

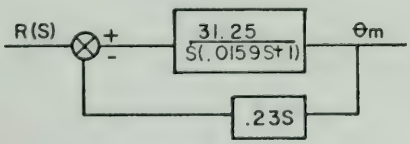

Using (11),

$$\frac{\theta_M(S)}{R(S)} = \frac{3.834}{S(.00195S + 1)} \qquad (12)$$

Now the inner loop may be replaced by (12) and the original controller takes the following form:

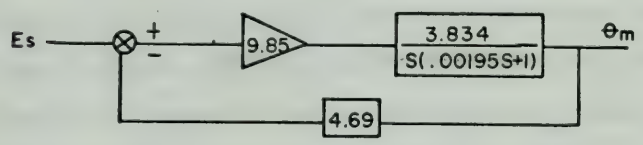

Using (11) again

$$\frac{\theta_M(S)}{e(S)} = \frac{\dfrac{3.834 \times 9.85}{S(.00195S + 1)}}{1 + \dfrac{3.834 \times 9.85 \times 4.69}{S(.00195S + 1)}}$$

Simplifying yields,

$$\frac{\theta_M(S)}{e(S)} = \frac{19364}{S^2 + 512.8S + 90820.5}$$

Noting the denominator to be of the form

$$S^2 + 2\zeta\omega_n S + \omega_n^2$$

the natural frequency and damping ratio are now easily found to be

$$\omega_n = 301.4 \text{ rad/sec (48 Hz)}$$

$$\zeta = 0.85 \ .$$

APPENDIX D - GUST GENERATOR FLOW FIELD

In order to study the flow field produced by the gust generator the previously described sensing vane was employed. In this manner, for fixed vane location, both steady state and oscillatory gust angles could be determined. Figure 19 shows the results of a survey made at varying distances upstream of the oscillator. As can be seen, vane angle maximum deflection appears to fall off linearly with frequency. Figure 20 shows the fall off in vane angle as distance upstream of the oscillator is increased. This survey was made in the same horizontal plane as the gust generator, Traces of the vane signal showed a clear sinusoidal signal regardless of oscillator frequency or horizontal position, indicating the lack of high frequency turbulence.

This was in marked contrast to the flow field which was found to exist downstream. In this region the basic sinusoidal motion produced by the oscillator was mixed not only with turbulent eddies from the oscillator assembly but also from direct jet impingement of the oscillator on the vane.

Figure 21 shows the variations in vane amplitude with frequency and position. The large variations in vane angle with frequency are probably due more to the large random variation in the output trace than any dominant physical trend. This made accurate data reduction difficult and perhaps the only conclusion that should be drawn from figure 21 is that the downstream gust field is turbulent and only mildly frequency dependent.

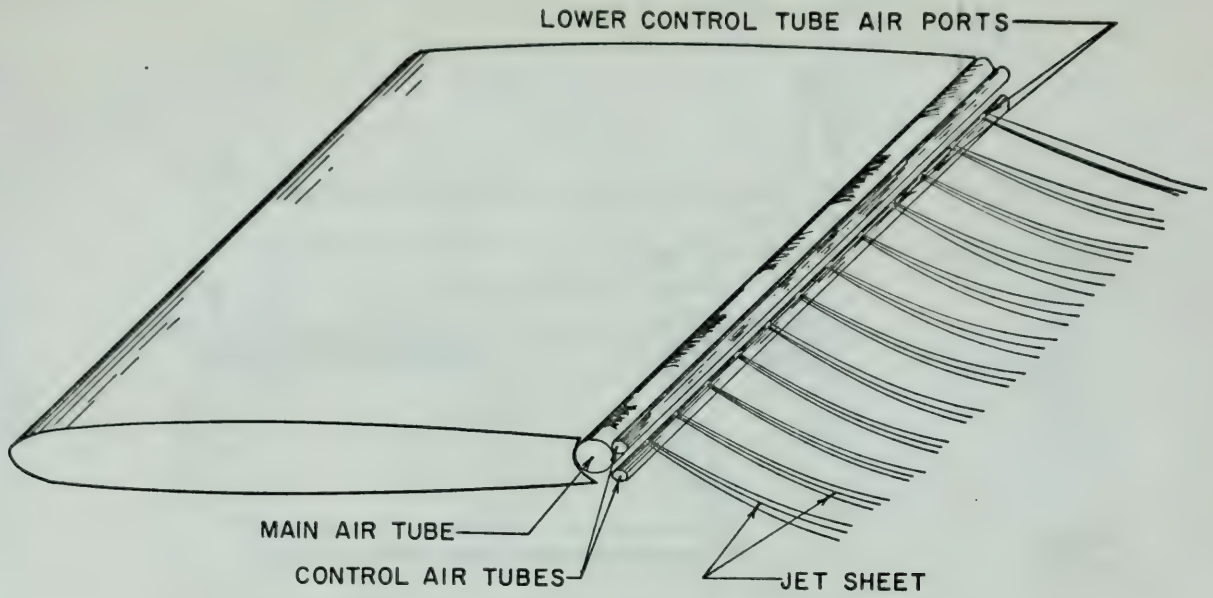

IN FIGURE ABOVE MAIN SHEET OF AIR IS DEFLECTED DOWNWARD BY AIR EJECTED DOWNWARD FROM UPPER CONTROL TUBE AIR PORTS

Figure 1
Jet flap showing blowing through top control tube.

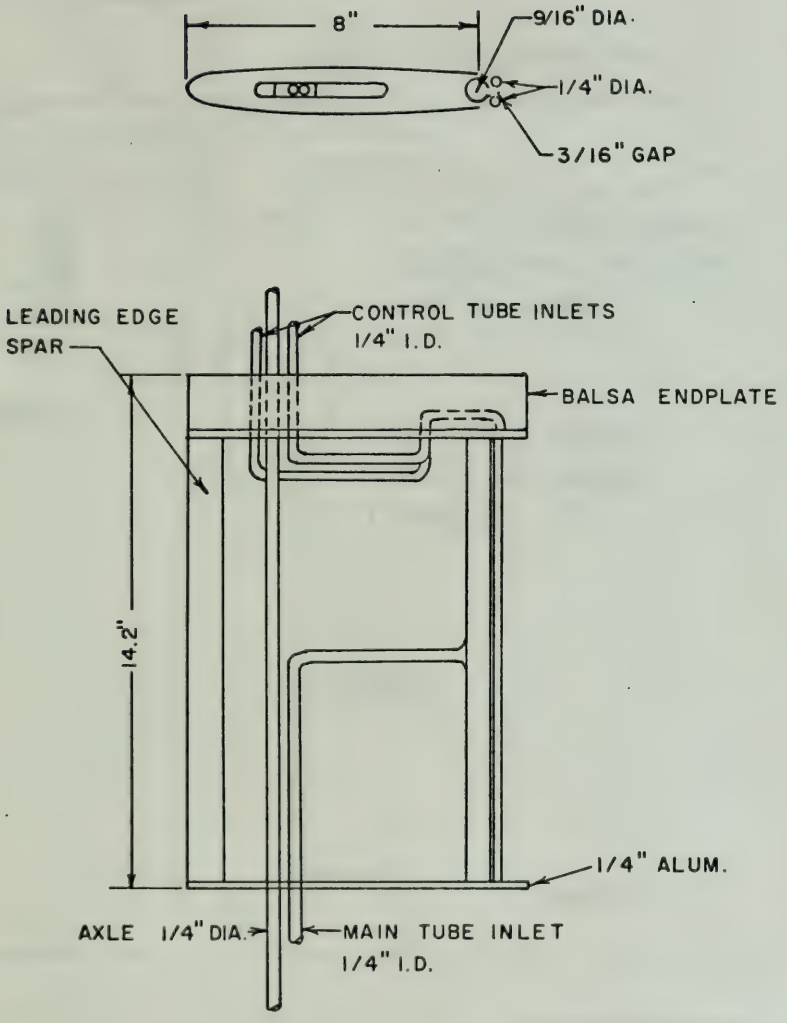

Figure 2
Internal construction details of jet flap.

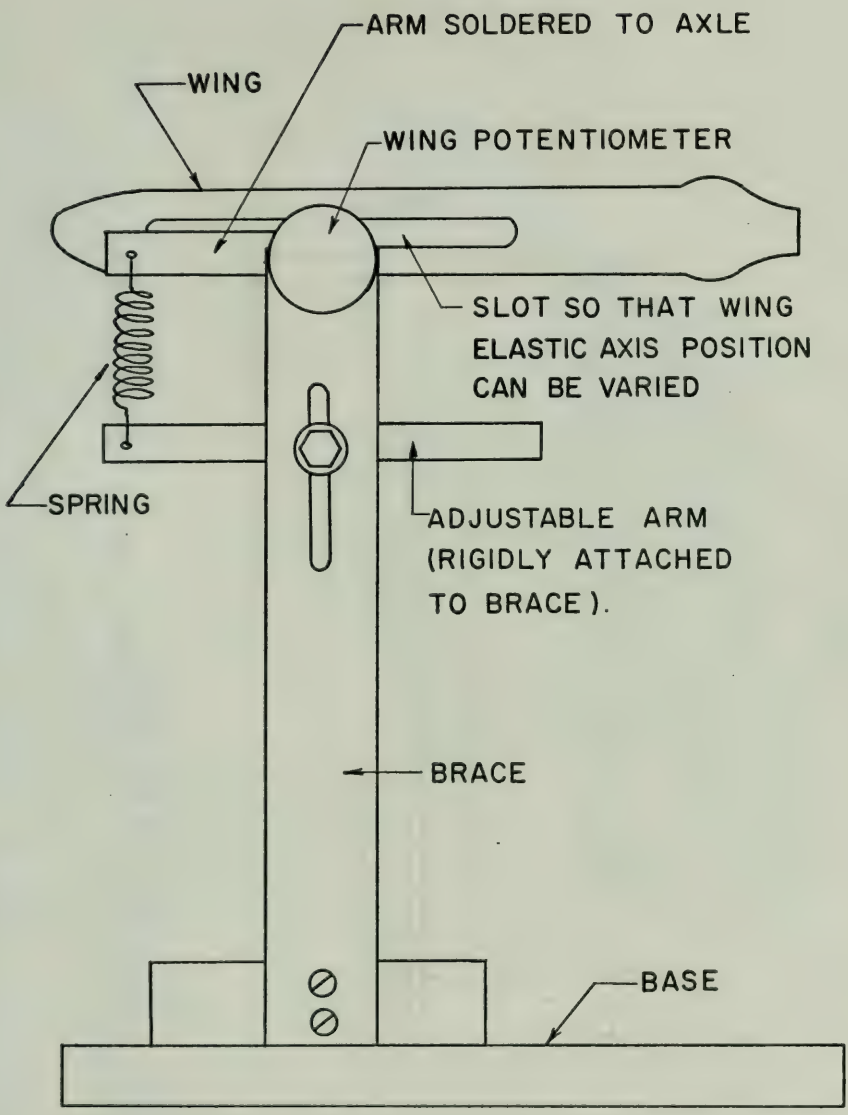

Figure 3
Wing mounting system to provide torsional oscillation.

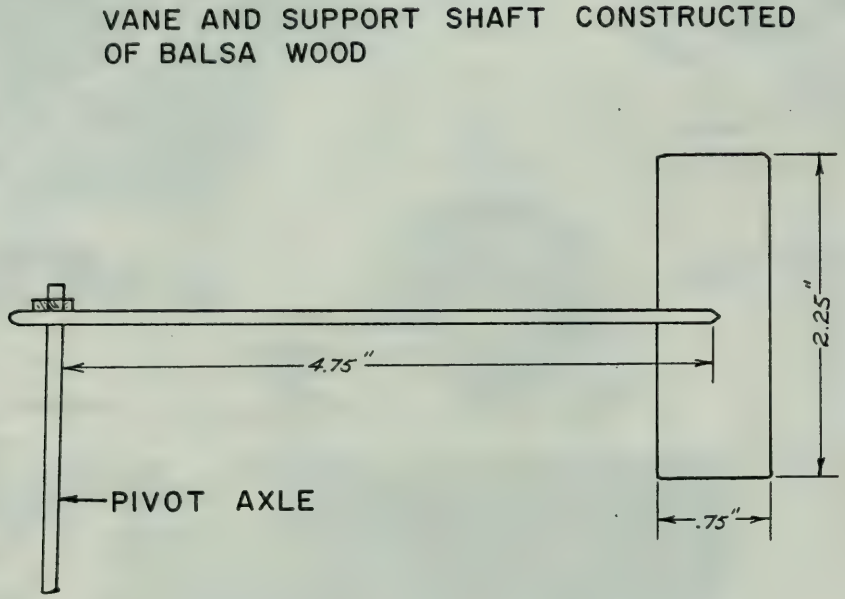

Figure 4
Sensor vane - top view.

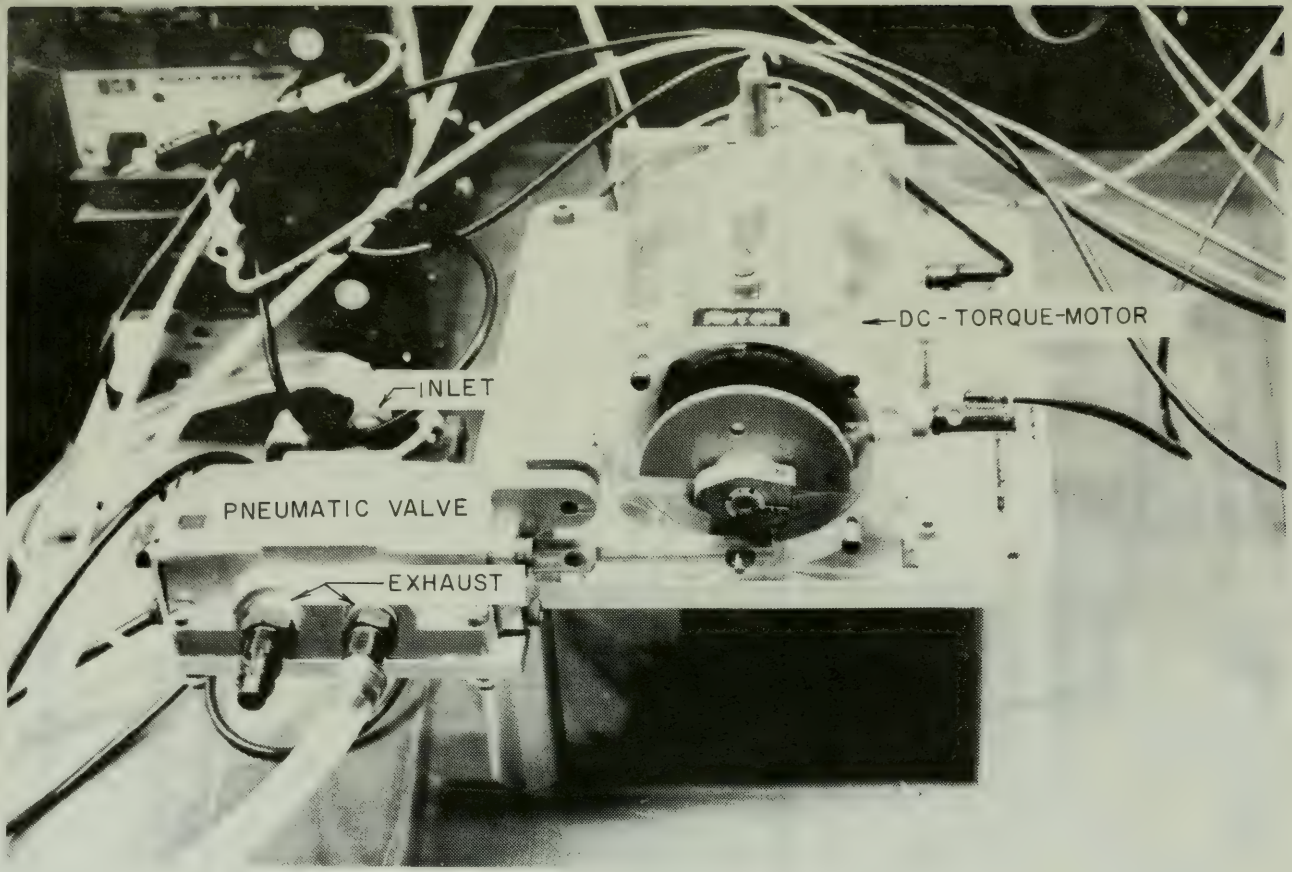

Figure 5
Servo motor with pneumatic valve attached.

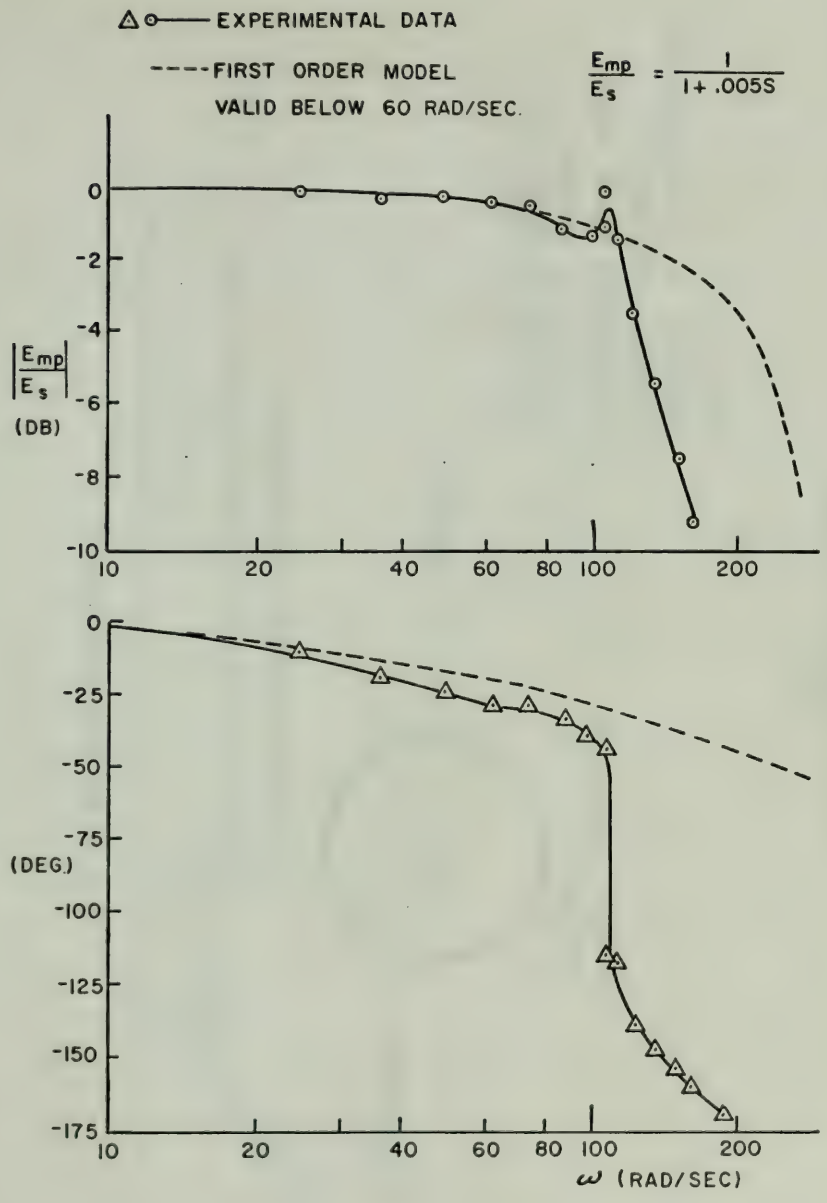

Figure 6
Magnitude and phase angle plots for servo motor.

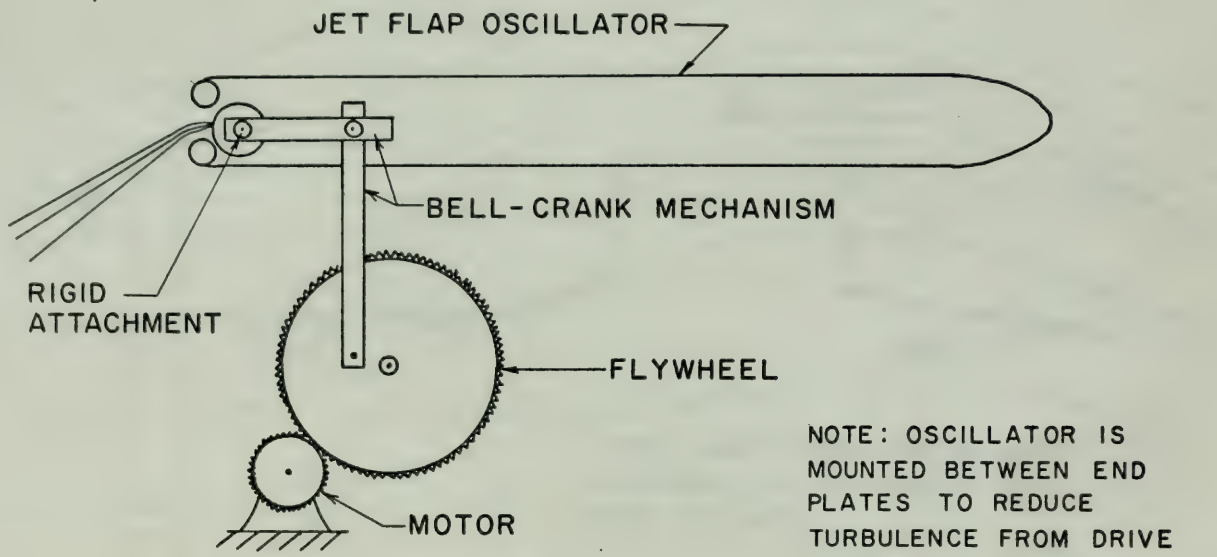

Figure 7
Oscillator construction schematic.

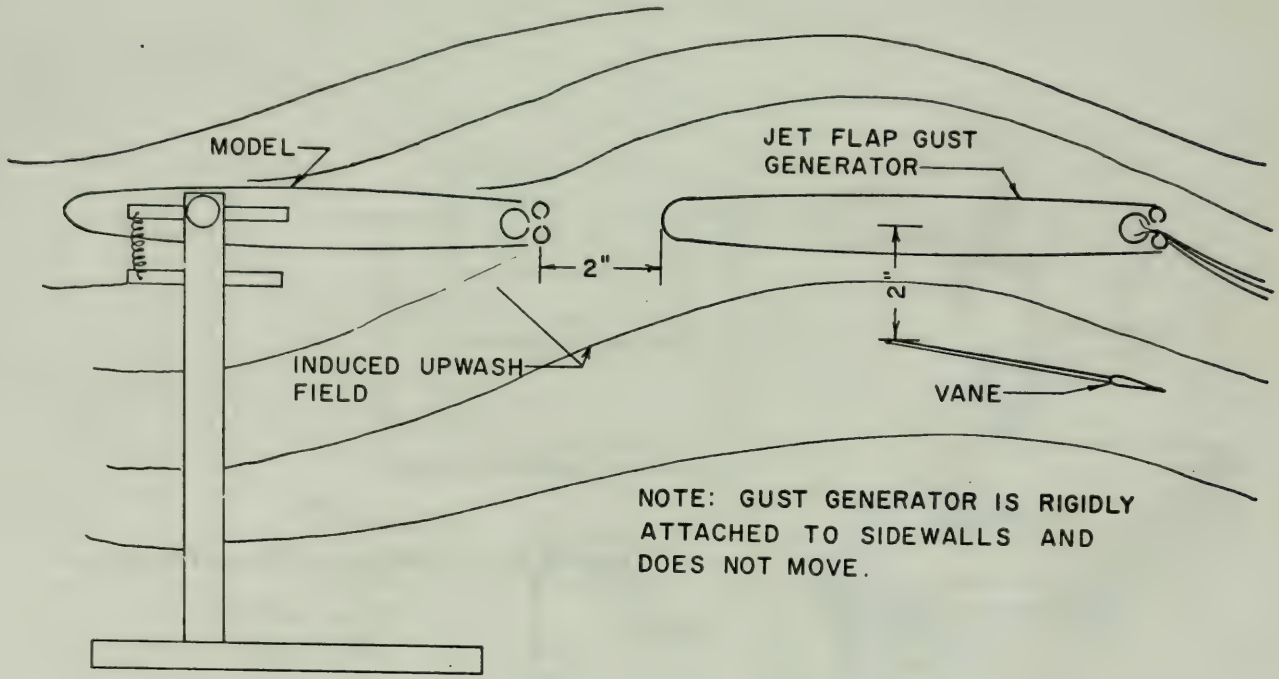

Figure 8
Configuration A test setup.

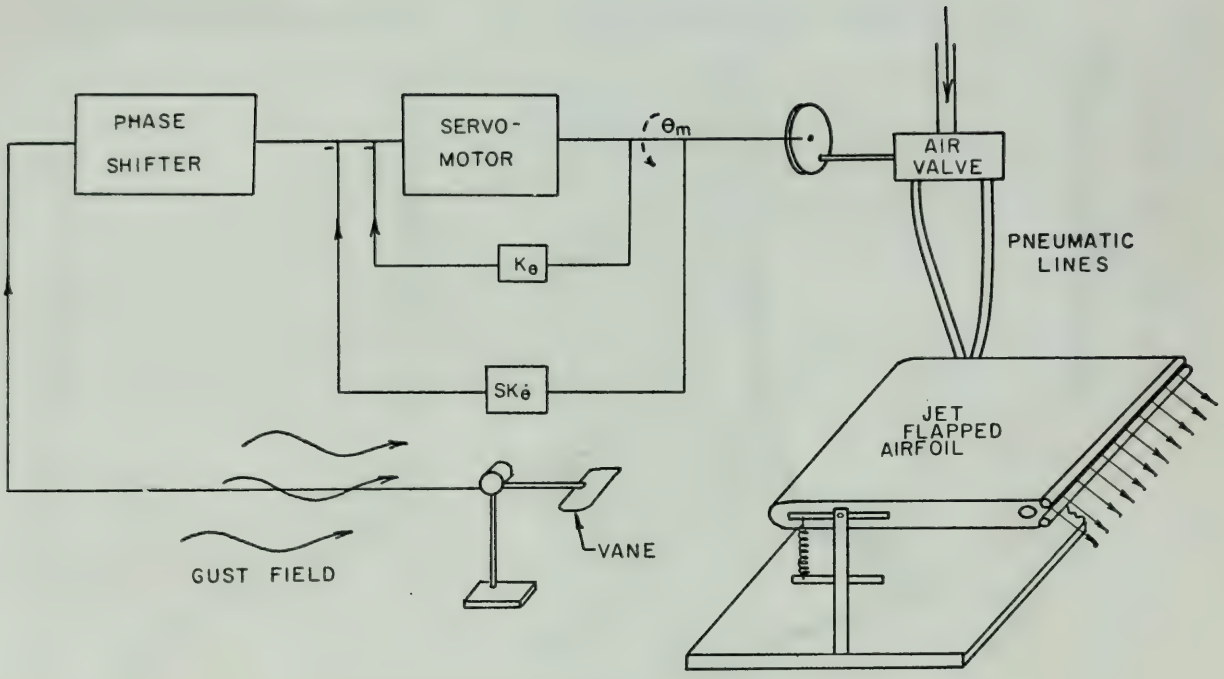

Figure 9
Control system block diagram.

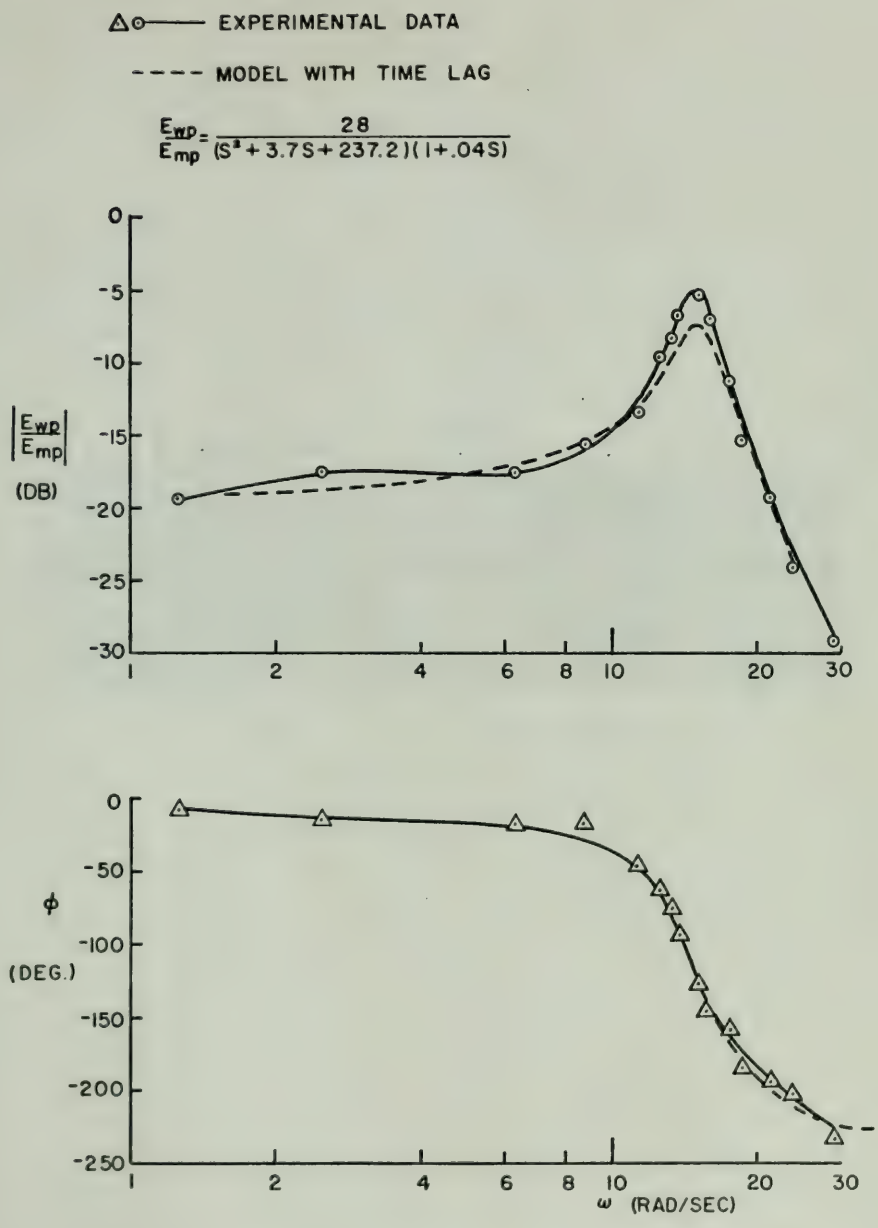

Figure 10

Magnitude and phase plots of wing position to motor position transfer function.

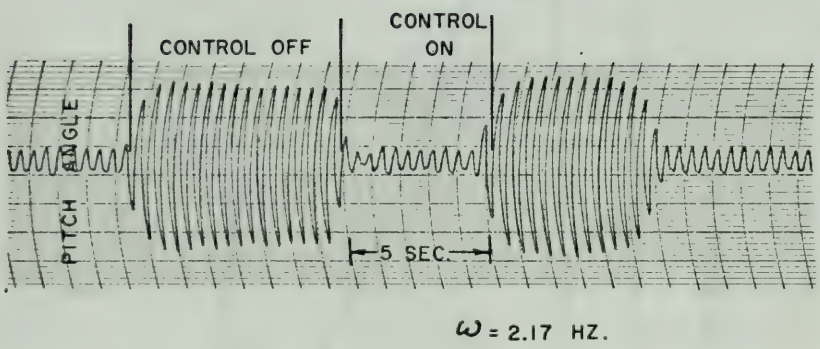

Figure 11
Configuration A wing response at 2.17 Hz with control off and on.

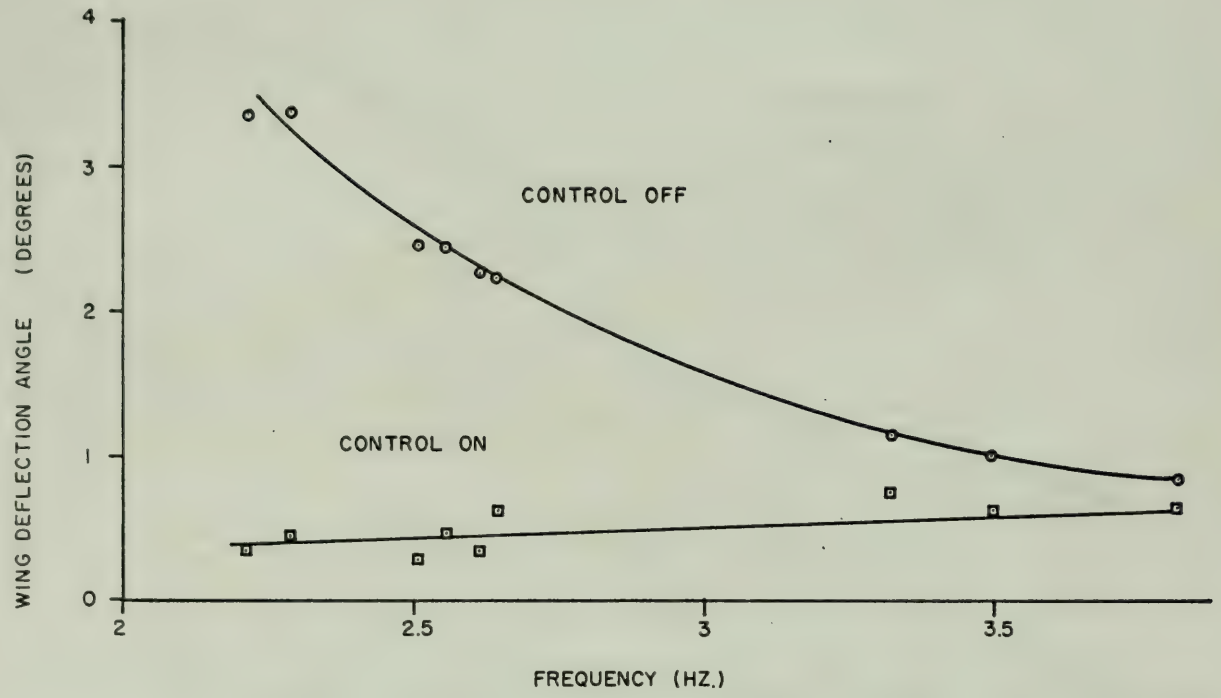

Figure 12
Plot of wing deflection angle versus frequency for control off and then on - configuration A.

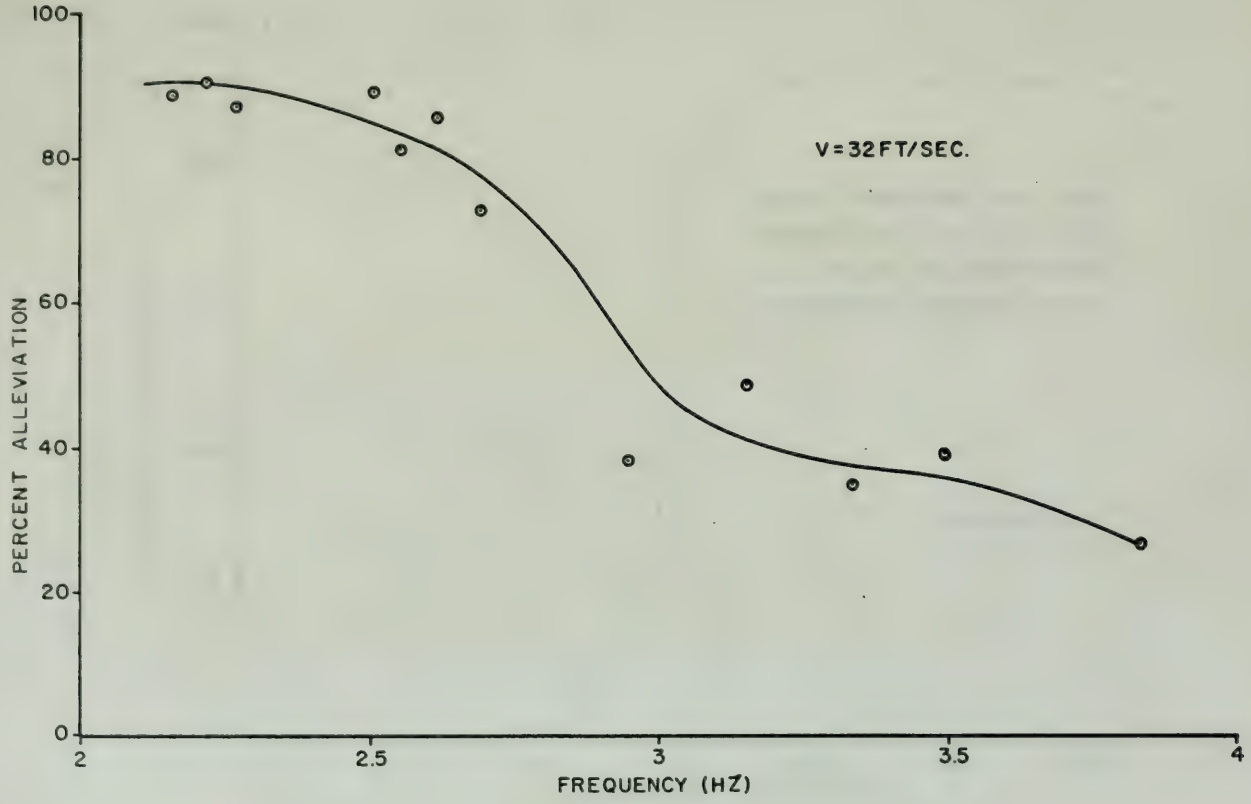

Figure 13
Plot of percent alleviation versus frequency - configuration A.

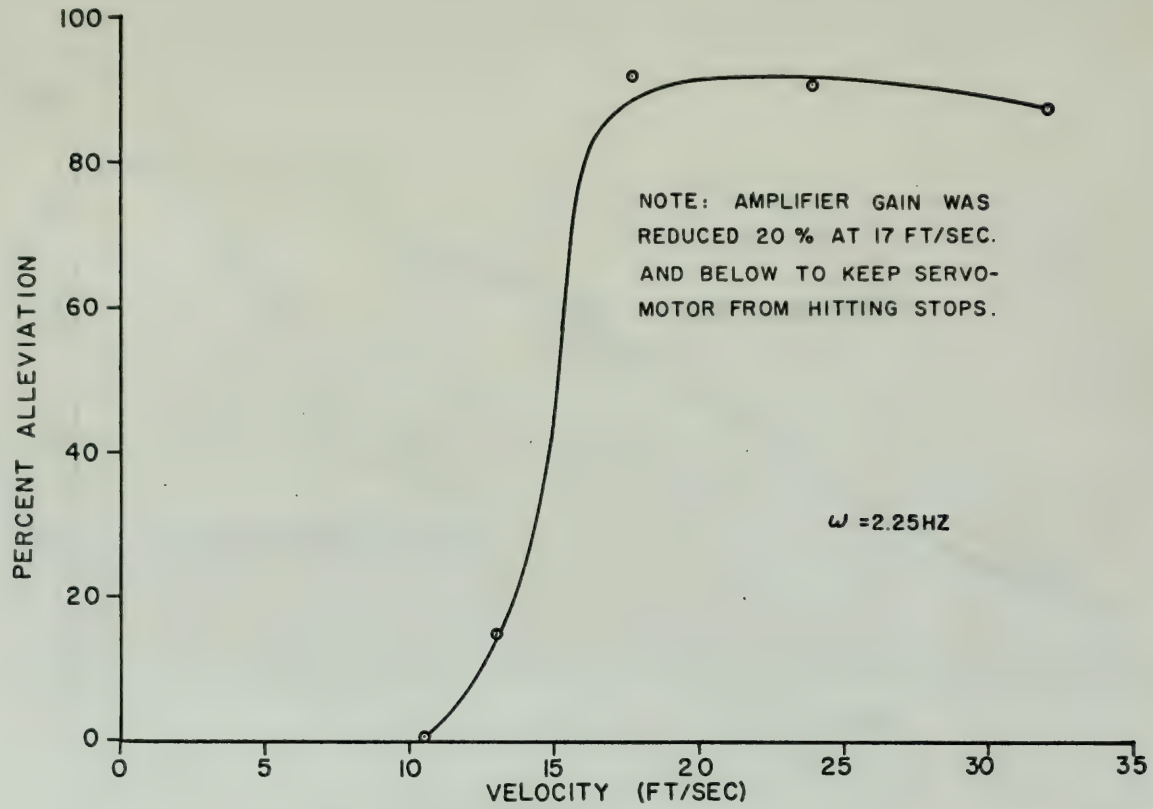

Figure 14
Plot of percent alleviation versus velocity - configuration A.

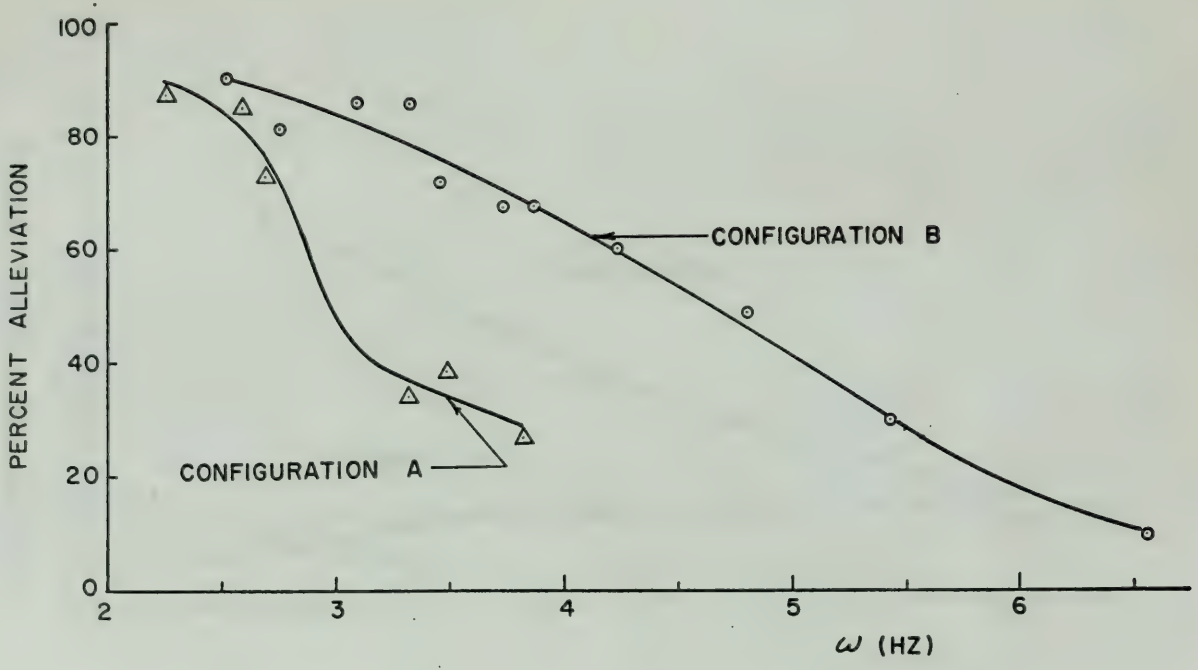

Figure 15
Plot of percent alleviation versus frequency - configuration A and B.

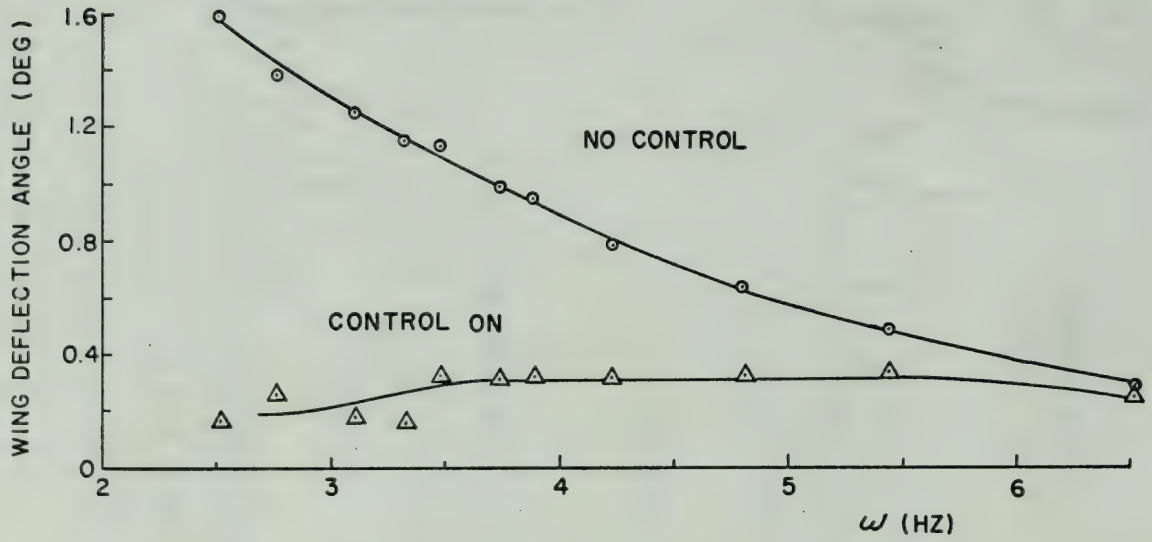

Figure 16
Plot of wing deflection angle versus frequency for control off and control on.

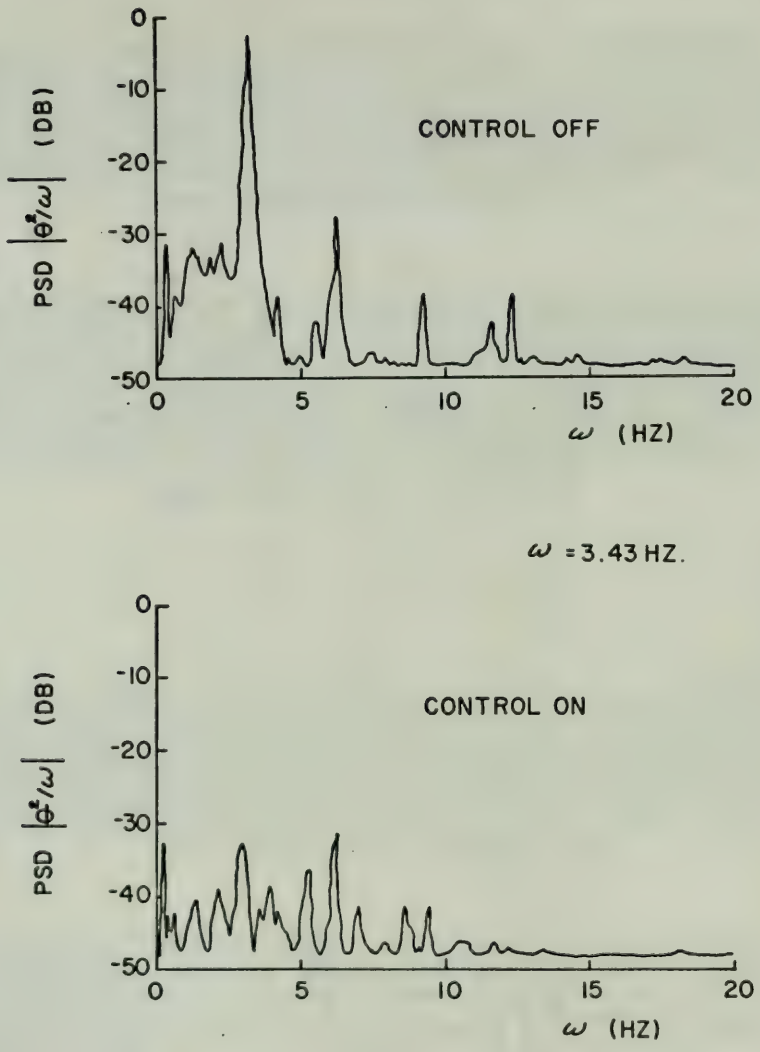

Figure 17
Power spectral density plots for a 3.43 Hz gust excitation with control off and control on.

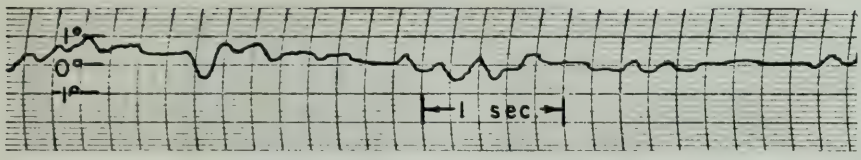

WING RESPONSE - CONTROL ON

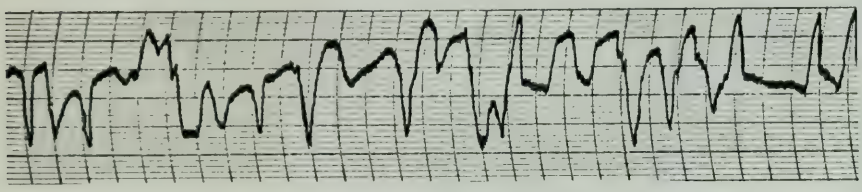

VANE RESPONSE - CONTROL ON

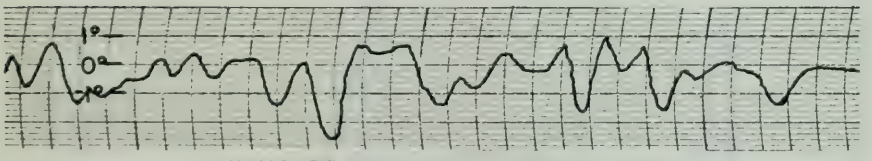

WING RESPONSE - CONTROL OFF

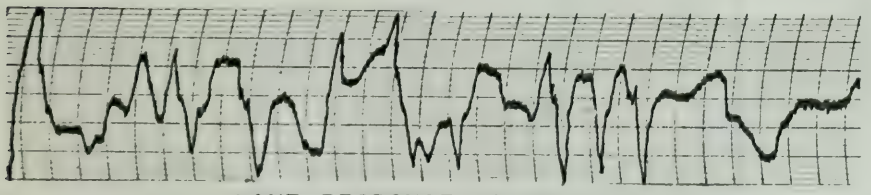

VANE RESPONSE - CONTROL OFF

Figure 18

Wing deflection angle versus time due to a random gust, control on and control off - configuration B.

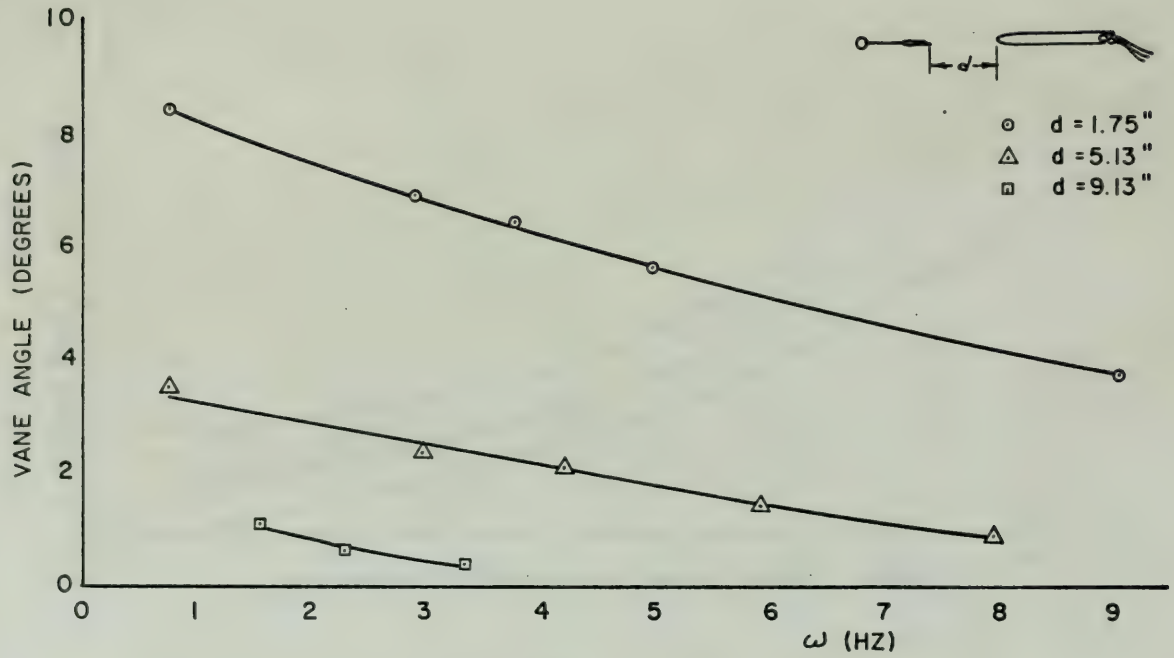

Figure 19
Vane angle versus frequency with distance upstream as a parameter.

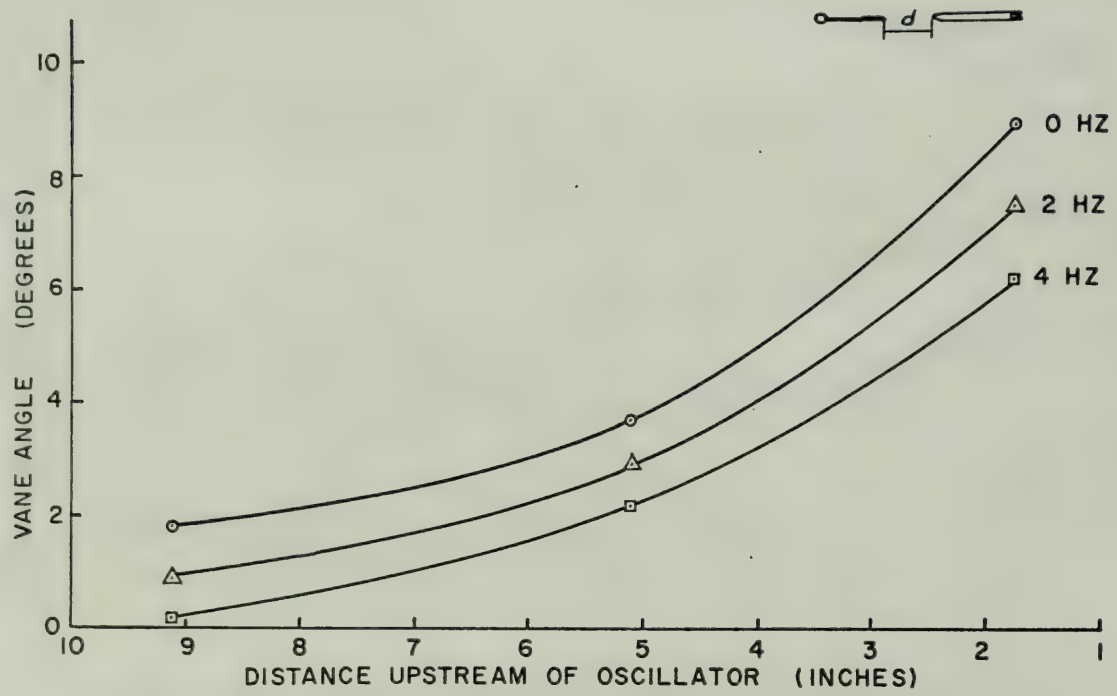

Figure 20
Vane angle versus distance upstream of oscillator with frequency as a parameter.

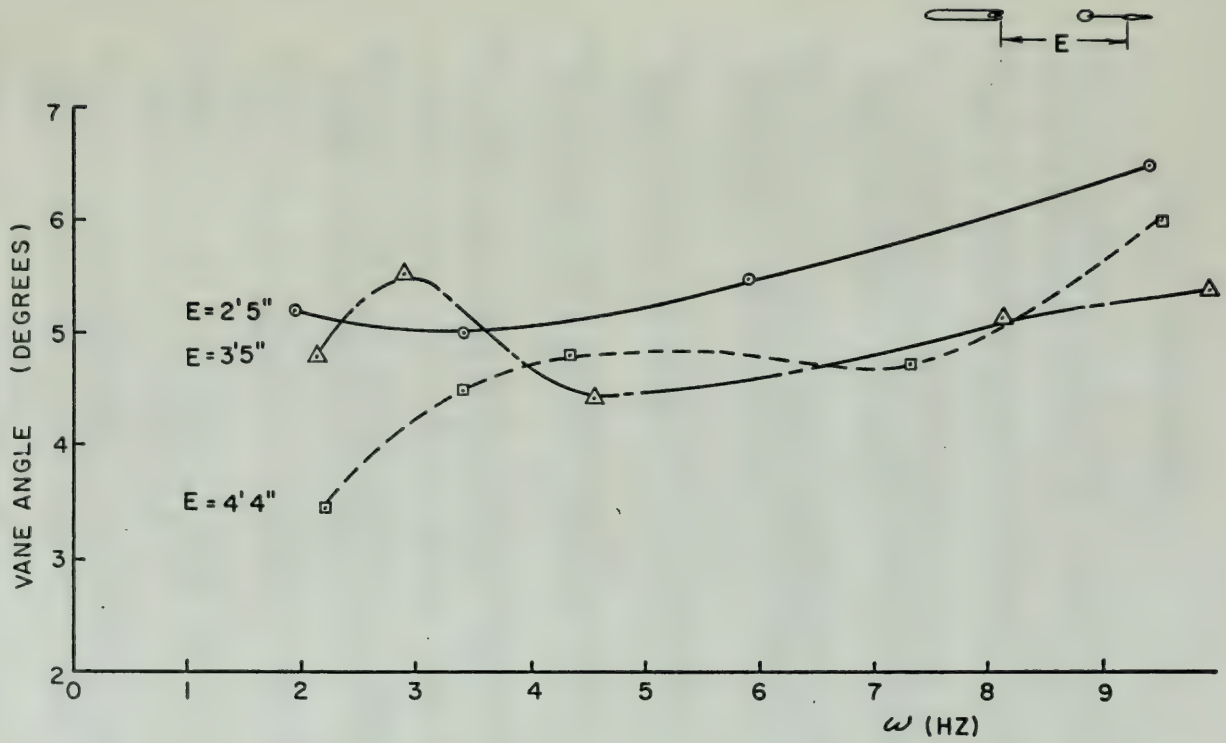

Figure 21
Vane angle versus frequency downstream of oscillator with distance as a parameter.

LIST OF REFERENCES

1. Andrew, G.M., Johnson, J.M. Jr., MIAS, Gardiner, F.H., "Gust Alleviator and Rigidity Augmentor for Supersonic Airplanes," Aerospace Engineering, May 1962.

2. NACA TN 3597, Analysis of a Vane Controlled Gust Alleviation System, by R.W. Boucher and C.C. Kraft, Jr., 1956.

3. North American Aviation, Autonetics Division AD 297945, EM 1163-104, Annotated Bibliography of Literature Concerning Gust Alleviation Techniques, Low-Altitude Turbulence and Related Topics, by B.A. Bryce, Feb. 1963.

4. NACA TN 3746, Initial Results of a Flight Investigation of the Wing and Tail Loads on an Airplane Equipped with a Vane - Controlled Gust Alleviation System, by T.V. Cooney and R.L. Schott, 1956.

5. A.F. Flight Dynamics Lab, AIAA Paper 66-997, Controlling Dynamic Response in Rough Air, by M.H. Davis and Dr. R.L. Swaim, Dec. 1966.

6. NASA TND-532, A Flight Investigation of an Automatic Gust - Alleviation System in a Transport Airplane, by P.A. Hunter and C.C. Kraft, Jr., 1960.

7. NACA TN-3612, Initial Results of a Flight Investigation of a Gust Alleviation System, by C.C. Kraft, Jr., 1956.

8. NASA SP-258, Gust Alleviation, by W.H. Phillips, p. 505-553, 1971.

9. NACA TN 2416, Theoretical Study of Some Methods for Increasing the Smoothness of Flight through Rough Air, by W.H. Phillips and C.C. Kraft, Jr., 1951.

9A. NACA TN 4056, Load Implications of a Gust Alleviation System, by W.H. Phillips, June 1957.

10. Cornner, R.J., Hawk, J., and Levy, C., "Dynamic Analysis for the C-47 Airplane Gust Load Alleviation System," Rept No. SM-14456, Douglas Aircraft Inc., July 29, 1952.

11. NASA TND-643, Flight Investigation of Some Effects of a Vane-Controlled Gust Alleviation System of the Wing and Tail Loads of a Transport Airplane, by R.L. Schott and H.A. Hamer, Jan. 1961.

12. Simmons, J.M. and M.F. Platzer, "Experimental Investigation of Incompressible Flow Past Airfoils with Oscillating Jet Flaps," AIAA Paper No. 70-79, Jan. 1970.

13. Swaim, R.L., "Aircraft Elastic Mode Control," Journal of Aircraft, Feb. 1971.

14. Thompson, G.O., Kass, G.J., "Active Flutter Suppression - An Emerging Technology," Journal of Aircraft, v. 9, no. 3, 1971.

15. Triplett, W.E., "A Feasibility Study of Active Wing/Store Flutter Control," Journal of Aircraft, v. 9, no. 6, 1971.

16. Wykes, J.H., "Structural Dynamic Stability Augmentation and Gust Alleviation of Flexible Aircraft," AIAA Paper No. 68-1067, Oct. 21-24, 1968.

17. ARC Tech Rpt., R and M no. 2972, Preliminary Report on a Gust Alleviation Investigation on a Lancaster Aircraft, by J. Zbrozek, K.W. Smith and D. White, 1957.

18. Inland Motor Corp., Direct Drive Servo Design, 1964.

19. North American Aviation, Data Systems Division, Technical Consideration in the Design of Gust Alleviation Control Systems, 17 April, 1967.

20. U.S. Army Transportation Research Command, Autonetics, Trecom Technical Report 64-1, Gust Alleviation Feasibility Study, April 1964.

21. Aircraft Load Alleviation and Mode Stabilization (LAMS), "B-52 System Analysis, Synthesis and Design". D3-7901-1, contract AF33(615)-3753, Sept. 1968.

22. McCloud, J.L. and Kretz, M., "Multicyclic Jet Flap Control for Alleviation of Helicopter Blade Stresses and Fuselage Vibration", Proceedings, Specialists Meeting on Rotorcraft Dynamics. Feb. 13-15, 1974.

23. Graham,D., "Automatic Control of Lateral Oscillatory Motion." Rpt No. TB-574-F-1, Cornell Aeronautical Lab, Inc. 1949.

24. Dimmock, N.A., "Some Further Jet Flap Experiments", National Gas Turbine Establishments, England, M. 225, 1956.

25. Stratford, B.S., "Early Thoughts on the Jet Flap", Aeron. Quarterly, Vol. 7, 45-59, 1956.

26. Spence, D.A., The Theory of the Jet Flap for Unsteady Motion, Journal of Fluid Mechanics, Vol. 10, Part 2, 1961.

INITIAL DISTRIBUTION LIST

		No. Copies
1.	Defense Documentation Center Cameron Station Alexandria, Virginia 22314	2
2.	Library, Code 0212 Naval Postgraduate School Monterey, California 93940	2
3.	Department Chairman, Code 57 Aeronautics Department Naval Postgraduate School Monterey, California 93940	2
4.	Professor M. F. Platzer, Code 57Pl Department of Aeronautics Naval Postgraduate School Monterey, California 93940	15
5.	Mr. R. Siewert Code AIR-320 Naval Air Systems Command Washington, D.C. 20360	1
6.	Mr. Bill Reed Aeroelasticity Branch NASA, Langley Field, Virginia	1
7.	LT Leonard J. Deal, Jr. 5514 W. 138th St. Hawthorne, California	2

REPORT DOCUMENTATION PAGE

READ INSTRUCTIONS BEFORE COMPLETING FORM

1. REPORT NUMBER

2. GOVT ACCESSION NO.

3. RECIPIENT'S CATALOG NUMBER

4. TITLE (and Subtitle)

An Experimental Study of a Vane Controlled Jet Flap Gust Alleviation System

5. TYPE OF REPORT & PERIOD COVERED
Master's Thesis;
March 1974

6. PERFORMING ORG. REPORT NUMBER

7. AUTHOR(s)

Leonard Joseph Deal, Jr.

8. CONTRACT OR GRANT NUMBER(s)

9. PERFORMING ORGANIZATION NAME AND ADDRESS

Naval Postgraduate School
Monterey, California 93940

10. PROGRAM ELEMENT, PROJECT, TASK AREA & WORK UNIT NUMBERS

11. CONTROLLING OFFICE NAME AND ADDRESS

Naval Postgraduate School
Monterey, California 93940

12. REPORT DATE
March 1974

13. NUMBER OF PAGES
77

14. MONITORING AGENCY NAME & ADDRESS(if different from Controlling Office)

Naval Postgraduate School
Monterey, California 93940

15. SECURITY CLASS. (of this report)
Unclassified

15a. DECLASSIFICATION/DOWNGRADING SCHEDULE

16. DISTRIBUTION STATEMENT (of this Report)

Approved for public release; distribution unlimited.

17. DISTRIBUTION STATEMENT (of the abstract entered in Block 20, if different from Report)

18. SUPPLEMENTARY NOTES

19. KEY WORDS (Continue on reverse side if necessary and identify by block number)

Gust Alleviation
Jet Flap
Turbulence

20. ABSTRACT (Continue on reverse side if necessary and identify by block number)

An experimental effort to demonstrate the feasibility of an active gust alleviator using a fluidically actuated jet flap control system was undertaken. The wing model had a variable deflection jet at the trailing edge and was free to move in pitch only. A vane mounted ahead of the wing served as gust sensor and provided the signal which controlled jet angle.

Experimental results showed the system capable of alleviating up to 92% of the motion caused by a sinusoidal gust at constant amplitude. RMS values of wing rotation angle were found to be 0.68 degrees with control off and 0.29 degrees with control on when excited by a random two-dimensional gust.

Thesis
D1826 Deal
c.1
150317
An experimental study of a vane controlled jet flap gust alleviation system.